SUBSOLIDUS PHASE RELATIONS IN THE SYSTEMS Ag-Sb AND Ag-Sb-S.

By

Sitaramayya Somanchi

A thesis submitted to the Faculty of Graduate Studies and Research of McGill University in partial fulfillment of the requirements for the degree of Master of Science.

Department of Geological Sciences

McGill University

August 1st, 1963.

Table of contents

Tables

Figures

Figure 7. Lattice dimensions versus composition curve for the ε phase in the system Ag-Sb. Solid solution limits are taken from Figure 5.

Figure 8. Composition versus d value curve for the ε' phase in the system Ag-Sb.

Figure 9. Lattice dimensions versus composition curve for the ε' phase in the system Ag-Sb. Solid solution limits are taken from Figure 8.

Figure 10. Isothermal section of the phase diagram of the system Ag-Sb-S at 400°C covering the region Ag-Sb-Ag_2S-Sb_2S_3.

Figure 11. Isothermal section of the phase diagram of the system Ag-Sb-S at 300°C covering the region Ag-Sb-Ag_2S-Sb_2S_3.

Figure 12. Partial solidus-liquidus relations along the pseudo-binary Ag_3Sb-$3Ag_2S.Sb_2S_3$ join.

Plates

Plate I. Antimonial silver (light grey) in ε phase. Specimen from Cobalt, Ontario (McGill collection 221 M1).

Plate II. Exsolution of ε phase (dark grey) in antimonial silver (light grey). Same specimen as Plate I.

Plate III. X-ray powder diffraction photos of

1) Synthetic antimonial silver (5.1 Wt.% Sb) annealed at 400°C, 10 days.
2) Specimen from Cobalt, Ontario (221 M1, McGill collection) containing ε phase and antimonial silver. Not annealed.
3) Synthetic ε phase (15.97 Wt.% Sb) annealed at 400°C, 10 days.
4) ε' Phase (24.01 Wt.% Sb) annealed at 400°C, 10 days.

Note: This is a contact print of the four films. On films 3 and 4, ink spots which appear as white dots, indicate the reflections caused by LiF which was used as an internal standard.

Abstract

The phase boundaries as obtained in the Ag-Sb system are as follows: Sb-rich solvus of ε phase at 500, 450, 400 and 350, and 300°C is 18.2, 17.7, 17.75 and 17.7 weight per cent Sb respectively. Ag-rich solvus of ε' phase (dyscrasite) at 500, and 450, 400, 350, 300°C is 22.5 and 22.9 weight per cent Sb respectively. Sb-rich solvus of ε' phase at 500, 450, 400 and 350°C is 27.2 weight per cent Sb and at 300°C is 26.9 weight per cent Sb. No inversion of ε' to ε'' at about 440-449°C was observed.

The homogeneity range of pyrargyrite is probably less than 1 weight per cent Sb_2S_3 at 400°C and in miargyrite less than 0.6 weight per cent Sb_2S_3 at 400°C.

Isothermal ternary sections at 400 and 300°C contain univarient assemblages as follows: α -Ag_2S- ε , Ag_2S- ε -pr, ε - ε'-pr, pr- ε'-my, my- ε'-Sb and my-Sb_2S_3-Sb. Two narrow two-phase regions were observed one connecting the Sb-rich side of the ε solid solution field to $3Ag_2S.Sb_2S_3$ (pr) and the other extending from ε' phase to $Ag_2S.Sb_2S_3$ (my). The two-phase region ε -pr has the same width at both 400 and 300°C. But the region ε' -my is wider at 300°C.

The occurrence of ε phase as a mineral at Cobalt, Ontario was confirmed by X-ray diffraction.

Acknowledgements

The experimental work was done in the laboratory equipped by Dr.L.A.Clark with funds from National Research Council (Grant A.1111).

The research was supported in part by Geological Survey of Canada Research Grant (NO.1-54) held by Dr.J.E.Gill, Dr.E.H.Kranck and Dr.V.A.Saull, which assistance is gratefully acknowledged.

I am sincerely thankful to my research director Dr.L.A.Clark for his guidance and for critically reading the manuscript.

I also wish to express my sincere thanks to Dr.A.J.Frueh, Jr. for his invaluable help in the X-ray work involved in this research.

I am also grateful to Dr.Gunnar Kullerud, Geophysical Laboratory, Washington for differential thermal analysis on two samples.

Chapter I

Introduction

In general a systematic study of synthetic minerals in the laboratory under different physico-chemical conditions can lead to a fuller understanding of the formation of the ore deposits. The factors governing the deposition and concentration of mineral deposits are many and varied; however, the relations between temperature, pressure, and mineral composition or assemblage can be predicted from laboratory experiments.

The solvus curves determined in the laboratory from a study of the synthetic minerals and a systematic study of the limits of composition of a given phase may be used in determining the temperatures of formation of ore minerals in nature. This information may also be used to get an idea of the physical and chemical conditions of the ore depositional environment. We may also be able to predict the bottoming of ore or the presence of a hidden shoot.

With this in view, work on the binary system Ag-Sb and the ternary system Ag-Sb-S was undertaken. These systems were investigated by previous workers, but the data was incomplete and not always accurate. Most of the previous observers have investigated the system Ag-Sb at temperatures above 400°C. No data was available at lower temperatures, and as this data was necessary for the investigation of the system Ag-Sb-S, further work in the system Ag-Sb was undertaken.

Of special interest, from a geological point of view, are the three phases in the Ag-Sb system, two of which occur as minerals. The existence of a mineral which is an equivalent of the ε phase in this system was overlooked by previous workers due to lack of accurate data. The other two minerals in this system are antimonial silver and dyscrasite.

Of the six sulphosalts of silver and antimony, miargyrite and pyrargyrite are the two most commonly occurring minerals. Information on these minerals could be of help in the study of the silver deposits.

The purpose of the present investigation of the Ag-Sb-S system was to determine the compatible mineral assemblages in isothermal sections at 400 and 300°C. In addition, the quasi binary system Ag_2S-Sb_2S_3 was also investigated, in part for solid solutions of possible use in geothermometry.

Chapter 2

Materials, Equipment and Techniques

Materials. The silver and antimony used in these experiments were obtained from the Consolidated Mining and Smelting Company. The silver (Cominco 59 grade, lot no. 2706) contains the following impurities in parts per million, Ca-0.1, Cu-0.2, Fe-4.0, Mg-0.1, Si-0.1. The antimony (Cominco 59 grade, lot no. 2473) contains one part per million As.

Sulphur, supplied by the American Smelting and Refining Company, (lot no. I02), has a purity of 99.999 + % and the impurities of Na and Cl are less than 1 ppm.

Methods of Synthesis. Most of the work was done using the simple sealed tubes of transparent silica glass with a 5 millimeter inside diameter. For larger charges, various diameters up to 7 millimeters were used. This glass was most suitable since its softening point is above 1600^{o}C, and its low thermal coefficient of expansion allows rapid cooling in cold water from high temperature. Reaction between the glass and the charges was never observed within the temperature range employed. The transparent nature of the glass allowed visual examination of the progress of reaction without opening the tube.

Extreme care was employed while loading the tubes. Each reagent was initially weighed out on a balance and put in the silica glass tube, which had previously been sealed at one end. Any material adhering to the walls was partially freed by gentle tapping. The glass tube was then left standing for a few minutes,

and most of the remaining material adhering to the walls was freed by tapping the tube again. By leaving the tube untouched for a few minutes some of the static electricity was dissipated from the tube, which was the main reason for the material sticking to the walls. The tube was then weighed. The next reagent was weighed on a watch glass and then loaded in the tube. The same procedure was adopted as above for freeing the material adhering to the tube walls. The tube was reweighed with every addition of the reagent, and, in this way the accurate weight of the reagents used was obtained. It was found this method minimized the errors due to loss during weighing. In most cases, after loading the tube, the tube was necked down to a capillary size just above the charge, with the sample end of the tube wrapped in a wet cloth to prevent heating and oxidation of the charge. Care was taken to leave as little space as possible in the tube above the charge. Where sulphur was used a small length of silica glass rod was placed on top of the charge to reduce the vapor volume before necking. The tube was then evacuated with a Cenco Hyvac vacuum pump to less than 0.001 mm Hg, after which the capillary was sealed with the torch (oxygen-commercial gas torch).

Temperature control and measurement. Equipment employed was similar to that described by Clark (1959). The runs were heated in horizontal, cylindrical electric furnaces. The furnace has an 18 inch long metal shell with 10 inch diameter transite ends and is filled with powdered magnesia. The core

consists of concentric alundum tubes with a concentric 6 inch long nickel plate between them to distribute the heat uniformly. The inside diameter is one inch. The nichrome winding on the outer tube is more concentrated toward the ends to offset the greater heat losses at the ends. The total resistance is about 24 ohms at room temperature. This furnace has a constant temperature ± 1°C over a 3.5 inch interval measured at 600°C.

For temperature control, automatic controllers were used. The variac which was built into each controller was adjusted by a two phase electric motor. The motor was actuated by an unbalanced Wheatstone bridge. The six volt bridge circuit was composed of two fixed resistances, a manually set resistance, and a platinum sensing resistor wound in with the furnace winding. This type of regulator controlled the furnace temperature to ± 3°C.

Furnace temperatures were measured with chromel-alumel thermocouples. The temperatures were continually recorded on a 12 channel Daystrom recording potentiometer. The temperatures were verified with a Rubicon potentiometer using reference junction at 0°C.

Quenching and annealing techniques. The samples were first homogenized at 750°C for a period of from 6 to 12 hours, and they were then annealed for a period of 10 to 24 days at the temperature of the run. They were removed from the horizontal cylindrical furnaces using long tongs, and were dropped

directly into a cold water bath. To minimize cooling of the run while transferring the tube from the furnace to the cold water bath, the tongs were held for a few seconds in the furnace above the sample.

Identification of the products. (a) Reflecting microscope. After opening the tube a portion of the charge was mounted and polished for study under the reflecting microscope.

In air many of the phases were too similar to be differentiated; however, using an oil immersion lens colour contrast was sufficient to distinguish all the phases. The phase boundaries obtained by this method are in general agreement with those obtained by X-ray methods. This method was also found useful in the study of the system Ag-Sb-S. Different phases in this system were sometimes difficult to identify and iridescent filming of the polished section was useful in some instances (Gaudin and McGlashan, 1938). A solution of 1 part 2 percent iodine in methyl alcohol added to 1 part of conc. H_2SO_4 by volume was employed.

A portion of the original charge was retained for X-ray study. Approximately 20 mg of the powder was utilized to prepare the spindle for the X-ray camera (camera diameter 114.6 mm). The remainder was stored in a polyethylene vial. Whenever it was possible the material was ground to a fine powder in a mortar. In some instances, particularly in the silver rich charges in Ag-Sb system, it was not possible to grind the material. This necessitated filing the material,

and filing introduced strain which gave diffuse X-ray reflections. Therefore the filings were annealed in sealed evacuated glass capsules for a period of 6 to 48 hours, at the same temperature that the run had been heated. It was noticed that the filings of a sample in a two-phase region were not all of the same size. As a result of differential hardness one of the phases produces finer filings and these adhered to the paper, or to the glass tube, with consequent differential loss. This has the effect of producing only very faint patterns in the X-ray photograph for that particular phase. X-ray patterns obtained using the annealed filings were sharp. Silver-rich compositions seemed to require more annealing time to remove the strain.

Preparation of the sample. The method of preparation of the sample for X-ray camera is described by Azaroff and Buerger (1958) in Chapter 5.

Lithium fluoride was used as internal standard for measuring the reflections. All the reflections were measured with reference to the LiF lines spacings for which are given by Swanson and Tatge (1953). This method of measuring the lines was an improvement on the accuracy of the readings over the established methods and also saved time.

Copper radiation was used with a nickel filter and exposure time was 5 hours at 32 KV and 16 MA.

The differential thermal analysis equipment used in the

present investigations is similar to the one described by Kerr, Kulp, and Hamilton (1949). Essentially it consists of a furnace which can produce a maximum temperature of 1100°C and has a heating rate of approximately 12.5°C per minute. It is mounted vertically.

The specimen holders used are also modelled after the equipment referred to above. In the present case the thermocouples were inserted into a holder made of steatite into which two holes were drilled for the two thermocouples. These protrude on top of the steatite block so as to fit into the dimple at the bottom of the sample tubes. The samples were contained in sealed evacuated tubes described by Kracek (1946). The chromel: alumel thermocouples in the dimple were essentially surrounded by, but not in contact with, the sample. Galena was used as the inert sample.

Chapter 3

Previous work on the Binary Systems

The Ag-S system. The Ag_2S-Ag portion of the system was investigated by Friedrich and Leroux (1906), Jaeger and Van Klooster (1912), Bisett (1914) and Urazov (1915). Studies of the sulphur-rich portions of the system were not attempted because of the difficulty of retaining sulphur in the preparations at elevated temperatures. Kracek (1946) overcame this difficulty by constructing a special thermal analysis apparatus, and investigated the entire system. (See figure 1).

According to Kracek (1946), silver sulphide, the only compound in the system, is almost insoluble in sulphur. Liquid immiscibility in the sulphur-rich portion of the system extends from 0.35 to 64.0 atomic per cent Ag at 740°C. For compositions beyond Ag_2S there is a second region of liquid immiscibility with the two liquids of 68.9 and 94.2 atomic per cent Ag at 906° C. A eutectic with sulphur very nearly coincides with the melting point of this element, 115.2°C, while that with silver is at 804°C and 68.0 atomic per cent Ag.

Kracek (1946) reported two transitions in silver sulphide, the temperatures of which depend upon the presence of either excess sulphur or excess silver. The two mean limiting temperatures for the upper transition are 622 and 586°C while for the lower transition they are 177.8 and 176.3°C. In both cases the higher temperature corresponds with the presence of excess sulphur.

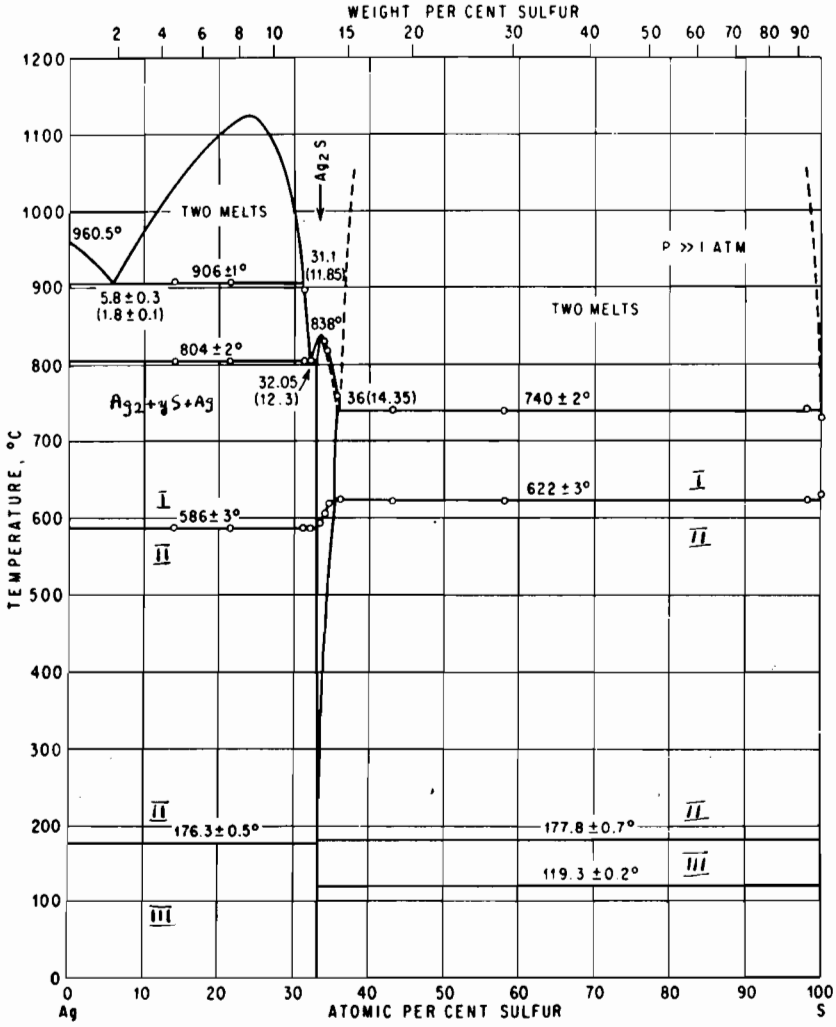

Figure 1: The temperature composition diagram of the system Silver-Sulphur (As compiled by Hansen, 1958).

He determined that silver sulphide melts and freezes congruently at 838 ± 2°C. The three sulphides of silver Ag_2S_2, Ag_2S and Ag_4S were synthesized by wet chemical methods (quoted by Kracek, 1946) but only Ag_2S occurs in the dry system.

In nature Ag_2S is found in two polymorphs, argentite (Ag_2S II) which is morphologically cubic, and the monoclinic acanthite (Ag_2S III) (Frueh, 1958), with the cell constants: a=4.23 Å, b=6.91 Å, c=7.87 Å, and β 99°35'. The transition at about 177°C is rapid and nonquenchable. As a result, the high temperature cubic form is never preserved at room temperature. Based on the crystal morphology, the deposition temperature can be determined relative to the transition temperature.

The Sb-S system. This system was investigated by Pelabon (1909), Jaeger and Van Klooster (1912), and Olie and Kruyt (1911-12).

The solidus temperature in the composition range 0-80 atomic per cent sulphur was found as 110°C, i.e., just below the melting point of sulphur at 115.2°C. The solid solubility of sulphur in antimony is about 0.3 atomic per cent based on measurements of electrical resistivity (Olie and Kruyt, 1911-12). It was not indicated if this represented a maximum value.

Two regions of liquid immiscibility of uncertain extent lie on either side of Sb_2S_3. Between about 1.5 and 21 weight (5.5-50 atomic) per cent sulphur the monotectic temperature was found as 615°C, and the eutectic at 520°C was placed at

about 24.5 weight per cent sulphur. The congruent melting point of Sb_2S_3 (28.31 weight per cent S) was determined as 555°C as compared with 546 and 554°C, according to Jaeger (1911-12), and Jensen (1947) respectively.

A second sulphide of antimony, Sb_2S_5, has been reported (quoted by Barstad, 1959) but was prepared only by wet chemical reactions.

The compound Sb_2S_3 occurs in nature as the mineral stibnite. Its orthorhombic structure is the prototype of $D5_8$ structure type with a=11.323 Å, b=11.323 Å and c=3.848 Å (Gottfried, 1929 and Hofmann 1933).

The Ag-Sb system. Charpy (quoted by Weibke and Efinger, 1940), conducted a microscopic examination of the Ag-Sb alloys and found a compound with a possible formula Ag_3Sb or Ag_4Sb. Heycock and Neville (1897) studied the liquidus and found that it consisted of three branches. The first break was at 25 atomic per cent Sb and corresponded to the compound Ag_3Sb. The second came at 40 atomic per cent Sb and corresponded to the eutectic at 485°C. The presence of a break at 25 atomic per cent was not considered sufficient evidence, however, to establish the above compound. Puschin (1907) studied this system and came to the conclusion from his electromotive force measurements, that antimony forms two compounds with silver, Ag_2Sb and Ag_3Sb. Petrenko (1906) found only one compound of the formula Ag_3Sb.

Broderick and Ehret (1931) investigated this system by

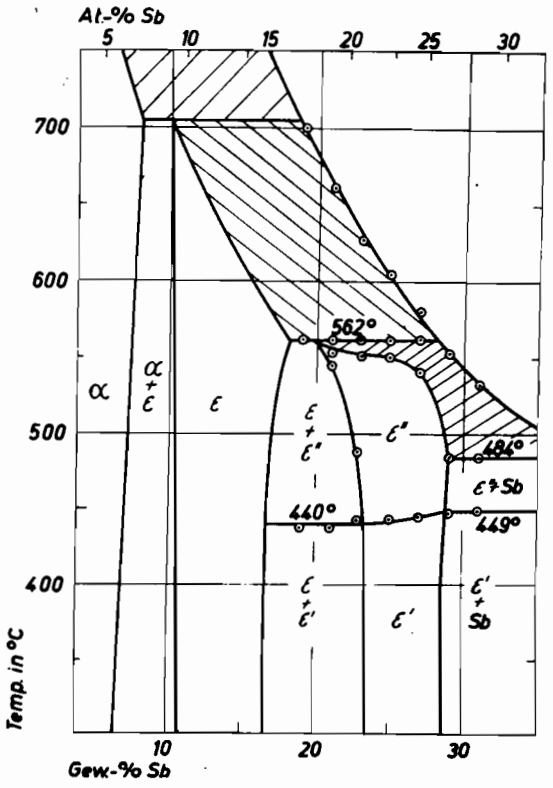

Figure 2: Partial phase diagram of the system Ag-Sb (after Weibke & Efinger, 1940).

X-ray examination and came to the conclusion that the maximum solubility of antimony in silver was about 6 weight per cent at room temperature. The solubility of Sb increases slightly with temperature being 7.1 weight per cent Sb at 470°C. The lattice parameter of silver in this phase increased from 4.084 Å for pure silver to 4.117 Å for the phase containing 6 per cent Sb. In the region between 11 and 16 weight per cent Sb, they observed a homogeneous hexagonal close packed phase. The size of the unit cell at 11 weight per cent Sb was a=2.926, b=c=4.784. They also noticed another homogeneous phase which is either rhombic or deformed cubic in the region between 22 and 28 weight per cent Sb. The size of the unit cell at 25.8 per cent Sb was a=3.006 Å, b=5.189 Å, and c=4.84 Å.

Weibke and Efinger (1940), in order to verify the results obtained by electro-chemical methods, investigated the system Ag-Sb, particularly in the region of 19 to 31 weight per cent Sb, by thermic, micrographic and X-ray methods. They made the alloys in an electric furnace in an atmosphere of dry purified nitrogen. The weight of the material taken was 30 gr. and samples were brought into equilibrium by heating at 500 and 400°C for 5 and 6 days, respectively, and then quenched in cold water. The amount of sample prepared for X-ray investigation was 5 gr. Their results are shown in figure 2.

<u>ε and ε′ phases</u>. Weibke and Efinger (1940) concluded that the Sb-rich phase boundary of ε phase is slightly inclined between 500 and 400°C, more antimony being taken into solid solution at higher temperatures. They fixed the saturation concentration of ε phase for Sb as 17.0 weight per cent at 500°C

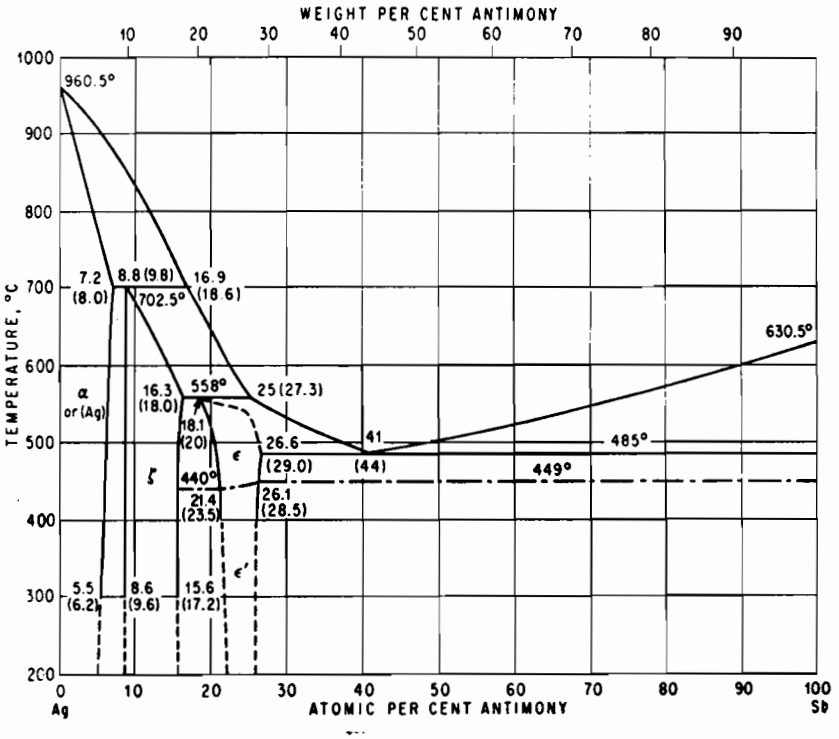

Figure 3: Phase diagram of the system Ag-Sb

(compiled by Hansen & Anderko, 1958)

and 16.7 weight per cent Sb at 400°C (see figure 2). Their figures for the average of the lattice constants of the alloys with 17.0 and 19.0 weight per cent Sb quenched from 500°C are: a=2.967 ± 0.002 Å, c=4.799 ± 0.004 Å, and from 400°C, a=2.962 ± 0.002 Å, c=4.787 ± 0.003 Å.

They also gave the phase boundaries of the ϵ' phase as 22.6 weight per cent at 400°C on the silver-rich side and as 28.6 weight per cent Sb at 400°C on the Sb-rich side. They observed a transition of the order-disorder type at about 440°C on the Ag-rich side and 449°C on the Sb-rich side.

The Ag-Sb relations were reviewed and compiled by Hansen and Anderko (1958) - (see figure 3).

The quasi binary system Ag_2S - Sb_2S_3. Of the six silver-antimony sulphosalts known, namely miargyrite ($Ag_2S.Sb_2S_3$), pyrargyrite ($3Ag_2S.Sb_2S_3$), polybasite ($9Ag_2S.Sb_2S_3$), pyrostilpnite ($3Ag_2S.Sb_2S_3$), stephanite ($5Ag_2S.Sb_2S_3$), and polyargyrite ($11Ag_2S.Sb_2S_3$), only two have been synthesized in the dry system Ag_2S - Sb_2S_3. These are pyrargyrite and miargyrite.

Gaudin and McGlashan (1938) in a pyrosynthesis of the system found five phases; miargyrite, pyrargyrite, argentite, stibnite, and a fifth phase "B" which was present in all bulk compositions with more than 73.3 atomic per cent silver sulphide and an excess of sulphur. Estimate of the volume of the different phases indicated that this phase "B" contained silver and antimony in atomic proportion 9 : 1.

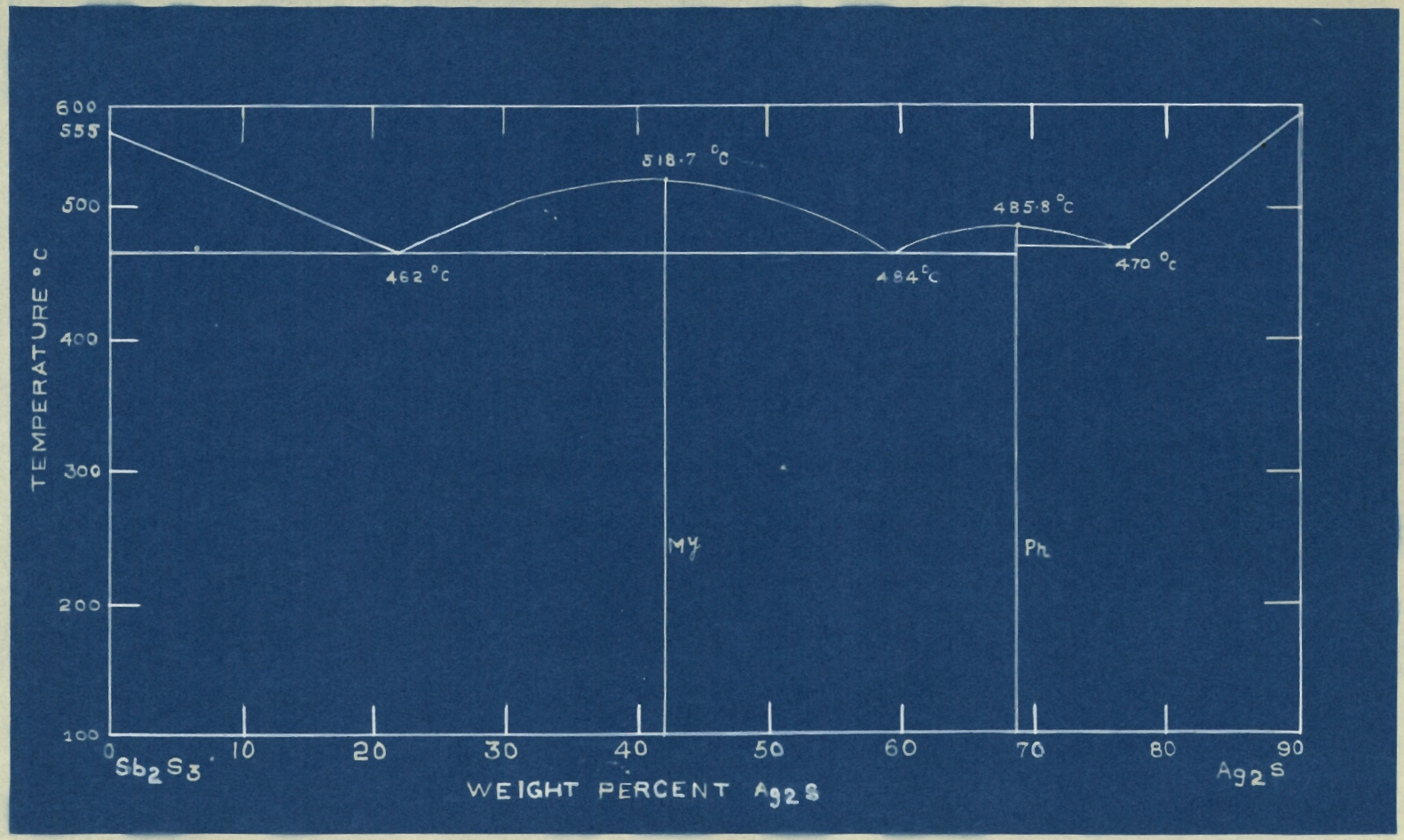

Figure 4: Phase diagram of the quasi binary system Sb_2S_3-Ag_2S
(After Jensen, 1947)

Schenk, Hoffman, Knepper and Vogler (1939) investigated the system by a method of isothermal reduction with hydrogen at 400°C. They concluded that the system contained the following intermediate compounds: $Ag_2S.Sb_2S_3$, $2Ag_2S.Sb_2S_3$, $4Ag_2S.Sb_2S_3$ and $49Ag_2S.Sb_2S_3$.

Jensen (1947) investigated this system in detail by d. t. a. methods (see figure 4). The melting point curve shows two maxima at 518.7 and 485.8°C, corresponding to the formation of the two compounds, $Ag_2S.Sb_2S_3$ and $3Ag_2S.Sb_2S_3$ respectively, with three eutectics at 462, 464 and 470°C, and 22, 59 and 77 weight per cent Ag_2S respectively. No extensive solid solution was found. He did not find any heat effect indicative of polymorphic transition in pyrargyrite. The crystal symmetry was determined by Harker (1936). The dimensions of the hexagonal unit cell are a=11.825 Å, and C=758 Å.

The compound Ag S.Sb S has two modifications. α $Ag_2S.Sb_2S_3$ is stable above 380°C. According to Graham (1951) the crystal symmetry is cubic with a lattice constant a-5.653 A. The transformation to the monoclinic low temperature modification β $Ag_2S.Sb_2S_3$, miargyrite, takes place on slow cooling; however, the high temperature form is preserved by rapid cooling.

Graham (1951) showed that crystal habit of naturally occurring miargyrite is in complete harmony with its crystal lattice showing no cubic pseudo-symmetry. He concluded that this mineral crystallized below the inversion temperature, and it is not a paramorph of the corresponding high temperature cubic

form. Constants of the monoclinic cell are, a=13.197 Å, b=4.399 Å, c=12.856 Å, $\beta = 98^{\circ}37\frac{1}{2}'$ and Z=8.

Attempts by Jensen (1947) to prepare any compound richer in Ag_2S than the compound $3Ag_2S.Sb_2S_3$ met with failure. He performed no experiments below 200°C. Synthesis of polybasite and pyrostilpnite was reported by Weil and Hocart (1953) by heating the components in glycerol.

Previous work in Ag - Sb - S system. The ternary system Ag - Sb - S was investigated by Schenck, Hoffman, Knepper and Vogler (1939), by measuring the H_2S/H_2 ratio during the reduction of sulphides of the quasi-binary system Ag_2S - Sb_2S_3 with H_2 at 400°C. From the staircase curves obtained they deduced the boundaries of two-phase and three-phase fields. They gave the composition of the silver-antimony sulphides as $Ag_2S.Sb_2S_3$, $2Ag_2S.Sb_2S_3$, and $4Ag_2S.Sb_2S_3$. But Jaeger and Van Klooster (1912) and Jensen (1947) in their thermal studies observed only the phases $Ag_2S.Sb_2S_3$ and $3Ag_2S.Sb_2S_3$.

Barstad (1959), re-examined the isothermal section of the phase diagram of the ternary system Ag-Sb-S at 400°C. In his investigations he obtained tie lines between Ag_2S and antimonial silver (α-phase) and between ϵ-phase and Ag_2S. He observed a narrow two-phase region whose tie lines connect $3Ag_2S.Sb_2S_3$ (pyrargyrite) and the antimony-rich end of the ϵ-phase solid solution in the Ag-Sb system. The tie lines from the ϵ'-phase (dyscrasite) are connected to $3Ag_2S.Sb_2S_3$ except for a narrow region on the antimony-rich side where the tie lines join with $Ag_2S.Sb_2S_3$ (αmy). He also indicated a tie line between Sb and

$Ag_2S.Sb_2S_3$. His ternary section utilized the Ag-Sb phase relations of previous workers.

Chapter 4

Experimental investigation of the Ag - Sb system

Work on this system was undertaken as a preliminary to the work on the ternary system Ag-Sb-S. As the liquidus and solidus relations were previously adequately determined, the present investigation was confined to the subsolidus region which is also of principal geological interest. Experiments were performed in the temperature range 300-500°C in the composition range 9 to 30 weight per cent Sb. Runs weighing 300 mg. were prepared for various compositions, were homogenized at 750°C and then annealed for a period of 10 days at the required temperatures.

General description of the phase diagram. Four solid solution phases have been recognized in this system (see figure 3) the α phase (antimonial silver), ϵ phase, ϵ' phase, and antimony.

The α phase has a solid solution limit of 8.0 weight per cent Sb at 700°C. At its incongruent melting temperature, 702.5°C, the ϵ phase has the composition 9.8 weight per cent Sb. The Ag-rich solvus of ϵ is relatively constant being 10.1 per cent at 400°C. The Sb-rich limit of solid solution occurs at 558°C and approximately 19.0 weight per cent Sb. The solid solution field becomes less extensive at lower temperatures. The ϵ' phase forms peritectically at 558°C and 20.0 per cent Sb. The solid solubility of Sb increases rapidly with decreasing temperature initially, but decreases

slowly below 500°C. Limits at 500°C are approximately 22.5 and 27.2 weight per cent Sb. The eutectic occurs at 44.0 weight per cent Sb, and 485°C. The solid solubility of Ag in Sb appears to be negligibly small (Broderic and Ehret, 1931, and Weibke and Efinger, 1940).

Vapour pressure. According to the Hand Book of Chemistry and Physics (1961), the vapour pressures of antimony and silver are 10^{-5}mm. Hg at 466°C and 10^{-5}mm. Hg at 767°C respectively. The present investigation of the Ag-Sb system is confined to the temperature range of 300 to 500°C where the vapour pressures of these two elements would be much lower.

The runs were sealed in evacuated glass tubes. Each run has its own vapour which at a given pressure is in equilibrium with the other phases at that temperature. Since the vapour pressures in the present experiments are very low and the vapour volume in the sealed capsules is relatively small, it is safe to assume that the loss of material from the solids to the vapour phase is negligible (i.e., $<<$ 0.01 per cent).

α phase. In my experiments the phase boundaries of the α phase and the ε phase on the silver-rich side could not be determined by X-ray study alone. In the two-phase region $\alpha+\varepsilon$, the powder photographs show a very strong pattern of antimonial silver, the lines of which are somewhat blurred and slightly drawn together. This blurring was first attributed to insufficient annealing for removal of strain induced by filing. However, no improvement was noticed after annealing the powder

for 48 hours at the temperature of the original run. Contraction of the pattern is due to an expansion of the silver lattice corresponding to the replacement of some of the atoms in the silver structure by the large atoms of antimony. According to Peacock (1940), if the distortion of the silver lattice is measured by the proportion of the replacing antimony, antimonial silver with 6½ per cent Sb will have a rhombohedral lattice with α 90°11'. A lattice so nearly cubic would give a cubic powder pattern with slightly blurred lines.

From polished sections it appears that 6½ weight per cent Sb is near the limit of the α phase solid solution field at 300°C. At the same temperature the Ag-rich ϵ solvus is at 10.1 weight per cent antimony. The lattice constant of antimonial silver with 5.1 weight per cent Sb is a=4.1112 Å as compared to a=4.119 ± 0.005 Å of antimonial silver with 6.78 weight per cent Sb (Peacock, 1940), and a=4.0933 Å for pure silver.

The results obtained during the course of the present investigation in the region α and $\alpha + \epsilon$ phases seem to agree with the results obtained by previous workers.

<u>ϵ phase</u>. A series of runs across the composition range 9 - 20 weight per cent Sb were prepared and equilibrated at 400°C. The samples were studied both microscopically and by X-ray diffraction methods (see table 1). From the X-ray powder photographs the d value versus composition curve was prepared (see figure 5). There is apparently a linear relation with

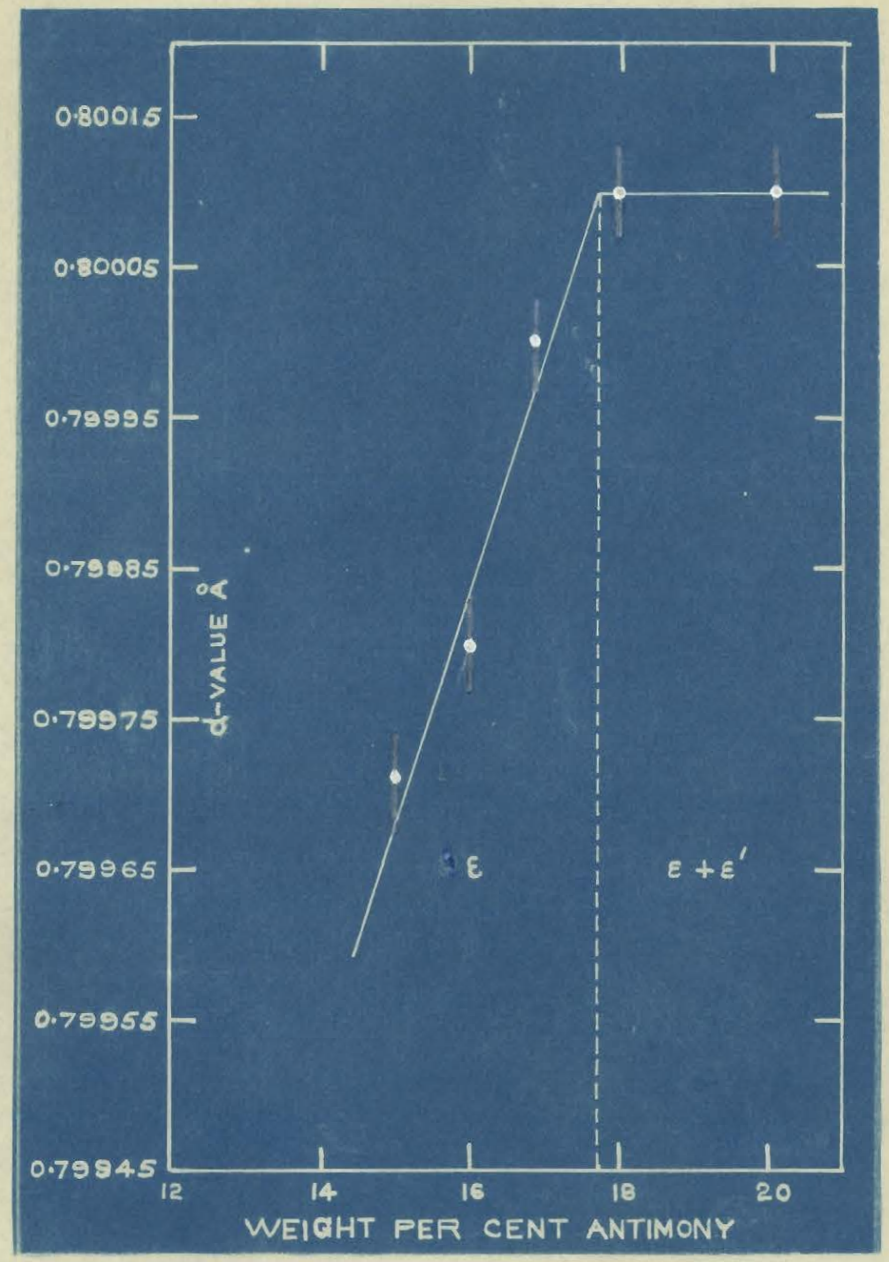

Figure 5: Composition versus d value curve for the ε phase in the system Ag-Sb. (Points indicated are accurate to ± 0.0003Å)

composition. The reflection utilized for this purpose is in the back reflection region. The line was taken to be a single reflection as it did not vary in width or split up during its occurrence over a wide range of compositions. The reflection was not indexed either by the previous workers or during the present investigation.

The d value versus composition curve could not be extended to the Ag-rich end of the solid solution field because the X-ray reflections for those compositions were too diffuse to measure. The sharp break in the slope of the curve at 17.7 weight per cent Sb marks the limit of solid solubility at 400°C.

In order to determine the Sb-rich solvus of the ε phase, compositions in the $\varepsilon + \varepsilon'$ field were heated sufficiently long for the compositions of the existing ε and ε' to approach equilibrium. Compositions of the saturated ε phase were then determined with the aid of the d versus composition relation (figure 5). Using this technique the determined compositions are accurate to $\pm$ 0.0003 Å. The phase boundaries at 500, 450, 350 and 300°C were determined from the X-ray studies of two alloys with 19.58 and 22.0 weight per cent Sb (see table 2) quenched from the temperatures mentioned. As shown in figure 6, the boundary shows a slight inclination. The boundary at 300°C is at 17.7 weight per cent Sb. It is at 17.75 weight per cent Sb at 400°C and agrees well with the results obtained by polished section study (see table 2). Above

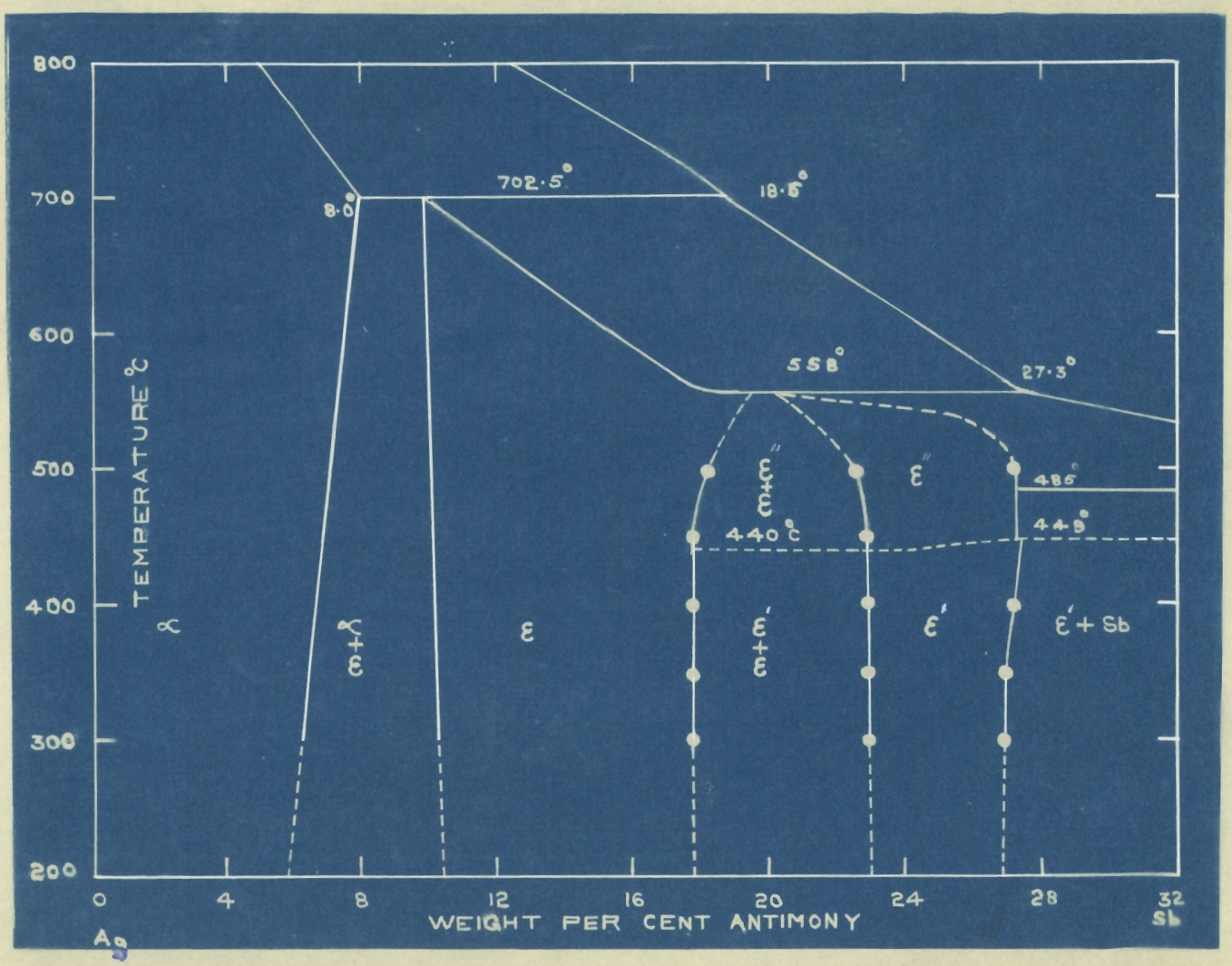

Figure 6: The temperature - composition diagram of the Ag rich portion of the system Ag-Sb.

Table 1

Table showing run compositions, d values, and the phases present in Ag - Sb experiments. Annealing time, 10 days at 400°C.

Composition Wt. % Sb	d value Å ± 0.0003 Å	Phases present X-ray and microscopic examination
9.0		α + ε + vapour
10.0		α + ε + vapour
14.3	0.79971 (ε)	ε + vapour
14.97		ε + vapour
15.97	0.79980 (ε)	ε + vapour
16.86	0.80000 (ε)	ε + vapour
17.99	0.80010 (ε)	ε + ε' + vapour
19.00	0.80257 (ε')	ε + ε' + vapour
20.00	0.80010 (ε) 0.80242 (ε')	ε + ε' + vapour
21.03	0.80252 (ε')	ε + ε' + vapour
22.03	0.80270 (ε')	ε + ε' + vapour
22.99	0.80260 (ε')	ε' + vapour
24.01	0.80427 (ε')	ε' + vapour
24.93	0.80580 (ε')	ε' + vapour
25.96	0.80740 (ε')	ε' + vapour
27.00	0.80905 (ε')	ε' + vapour
27.97		ε' + Sb + vapour
29.2	0.80932 (ε')	ε' + Sb + vapour
30.11	0.80930 (ε')	ε' + Sb + vapour

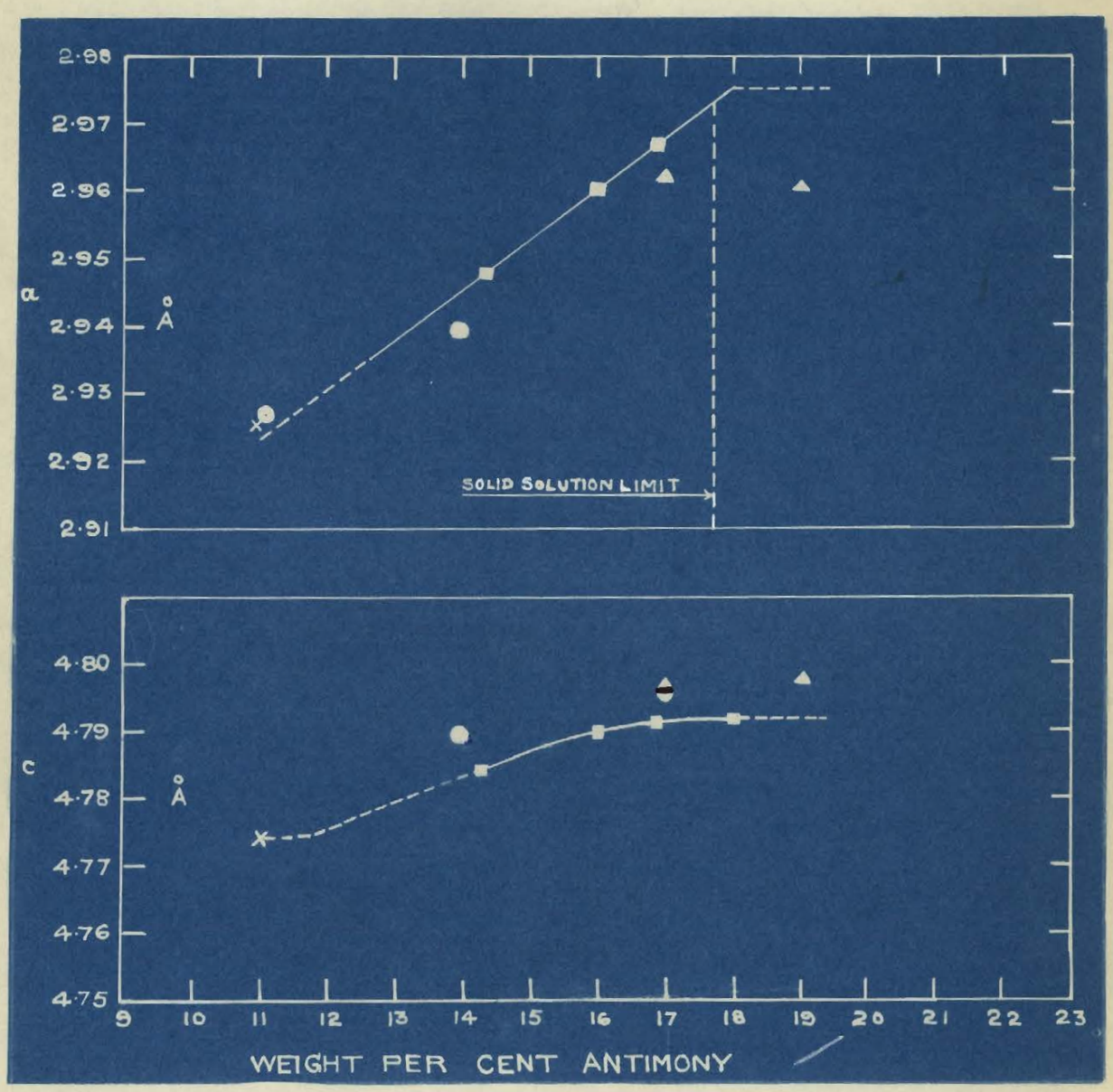

Figure 7: Lattice dimensions versus composition curve for the ε phase in the system Ag-Sb. Solid solution limits are taken from Figure 5.

× Broderick and Ehret.

○ Westgren, Hägg and Ericksson.

△ Weibke & Efinger.

□ Present investigation.

450°C the amount of antimony taken in solid solution increases relatively rapidly and at 500°C the phase boundary is at 18.2 weight per cent Sb.

The reflections in the X-ray photographs were indexed using the tables prepared by Broderick and Ehret (1931). The lines 201, 004 and 202 were utilised for calculating the lattice constants. The lattice parameters vary within the solid solution region. The linearity in the composition versus cell dimension curves is pronounced (see figure 7), particularly in the curve for a_o. The curve shows very good linearity as compared to the curves obtained by previous workers (Weibke and Efinger, 1940). The reasons are probably, (a) lack of equilibrium due to shorter annealing time in their runs, (b) oxidation of the material during the preparation of the runs (Skinner, Barton and Kullerud, 1959).

ε' and ε" phases. The peritectic transformation occurring at 558°C when cooling alloys with 18.5 to 28.0 weight per cent Sb, results in a new phase ε" from ε and liquid (Weibke and Efinger, 1940). ε" is a high temperature polymorph with the stable room temperature modification being designated ε'. The transformation of ε' to ε" occurs at 440°C on the Ag-rich side of the solid solution field, and at 449°C on Sb-rich side, according to Weibke and Efinger (1940). The average composition of this phase is Ag_3Sb and corresponds to the mineral dyscrasite.

A series of runs across the composition range 21 to 30 weight per cent Sb were prepared, melted and then equilibrated at 400°C. The samples were studied both microscopically and

Table 2

Table showing the runs used to determine the phase boundaries of the ε and ε′ phases. Annealing time, 10 days.

Composition Wt.% Sb	Temperature °C	Phases present	Phase boundaries Wt.% Sb	
			ε	ε′
19.58	300	ε + ε′	17.7	22.78
19.95	350	ε + ε′	17.75	22.9
19.95	450	ε + ε′	17.75	22.9
19.58	500	ε + ε′	18.2	22.5
28.3	300	ε′ + Sb	---	26.86
28.3	350	ε′ + Sb	---	26.9
28.3	415	ε′ + Sb	---	27.2
28.3	500	ε′ + Sb	---	27.2

by X-ray diffraction methods (see table 1). From the X-ray powder photographs the d value versus composition curve was prepared (see figure 8). As in the case of ε phase, there is apparently a linear relation with composition. The reflection utilized for this purpose has 2θ (Cu rad.) approximately 147 degrees. The line was taken to be a single reflection as it did not vary in width or split up in solid solutions over a wide range of compositions. The reflection was not indexed either by the previous workers or during the present investigation.

In order to determine the Ag-rich and Sb-rich boundaries

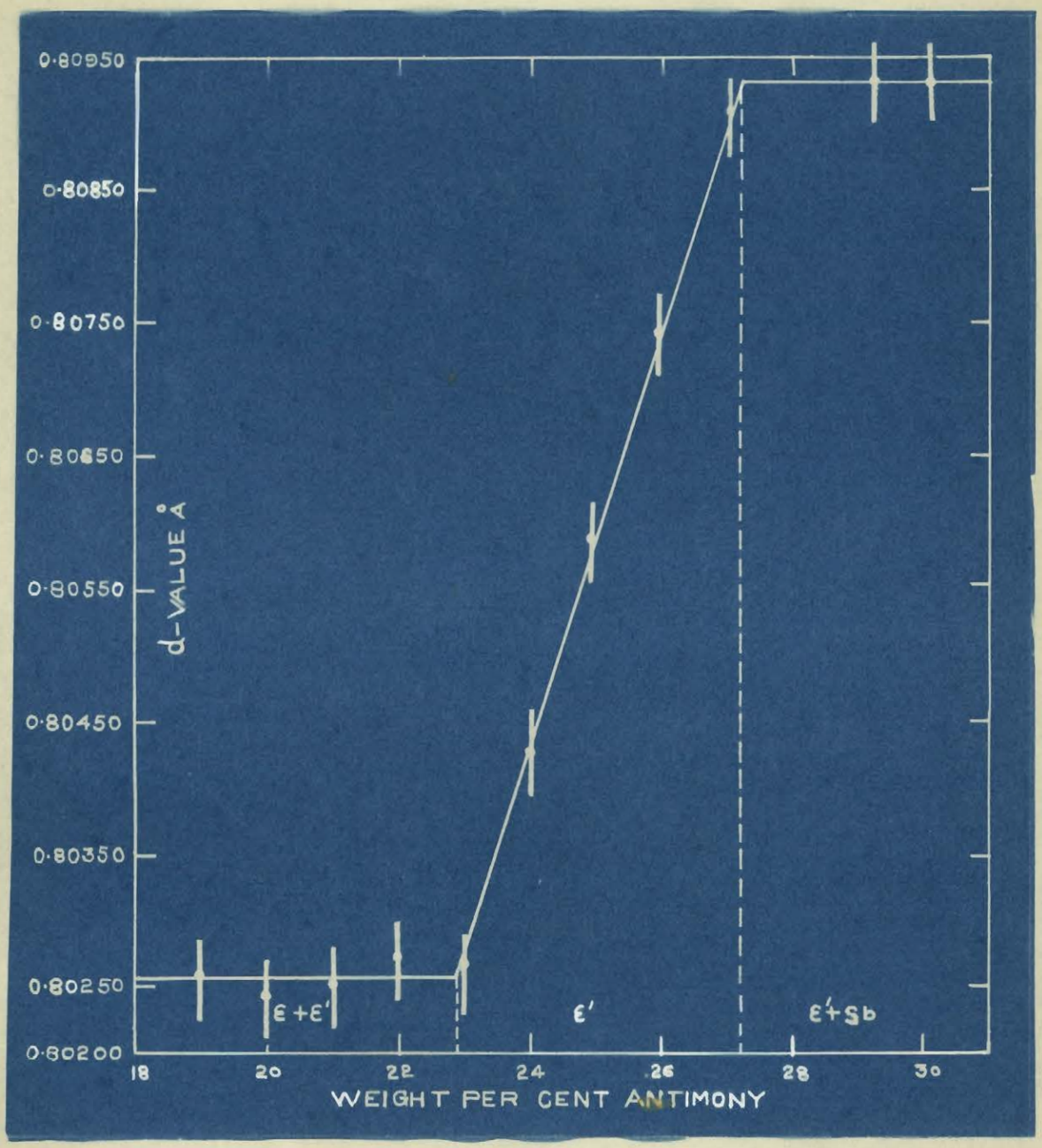

Figure 8: Composition versus d value curve for the ε' phase in the system Ag-Sb.

of the ε′ phase, compositions within the ε+ε′ and ε′+Sb fields were heated sufficiently long for the composition of the existing phases to approach equilibrium. Composition of the saturated ε′ phase was then determined with aid of the d value versus composition (figure 8) at 400°C.

The boundary of the ε′ phase on the Ag-rich side is 22.5 weight per cent Sb at 500°C and 22.9 weight per cent Sb at 450°C, 400°C, 350°C and 300°C. These compared with 22.6 weight per cent Sb at 500°C and 23.5 weight per cent Sb at 400 C as given by Weibke and Efinger (1940). (See table 2).

The Sb saturation boundary is 27.2 weight per cent Sb at 500, 450, 400 and 350°C, and 26.9 weight per cent Sb at 300°C as compared to 28.6 weight per cent Sb at 400°C obtained by Weibke and Efinger (1940), and 27.6 weight per cent Sb at room temperature as given by Westgren et al (1929) and Broderick and Ehret (1931). The solid solubility of antimony decreases slightly below 400°C.

The phase boundaries as fixed by microscopic study are in good agreement with the results obtained by X-ray study (see tables 1 and 2, and figure 8).

The inversion ε′ to ε″ occurs at 440°C in alloys saturated with silver and 449°C on the antimony side (Weibke and Efinger, 1940). Theoretically, a two phase region between ε′ and ε″ is necessary. The postulated break in the solvus on the Sb saturation boundary of the ε′ phase (see figure 6) could be the result if a transition really exists with a narrow two phase

region separating the two modifications.

Two samples with 15.06 (ϵ) and 25.03 (ϵ') weight per cent Sb were sent for differential thermal analysis to the Geophysical Laboratory, Carnegie Institute of Washington, to check for possible transitions. Neither the ϵ nor ϵ' phase showed detectable inversions. It may be that the ϵ' to ϵ'' transformation is an ordering process. Howevef, the X-ray powder patterns of these two phases are indistinguishable, giving rise to doubts about the actual existence of the transformation.

The area of solid solution as obtained in the present investigation is narrower than that obtained by Weibke and Efinger (1940). In their case the whole field was shifted towards antimony-rich side. This may be due to lack of equilibrium in their runs as a result of insufficient annealing, or to the effects of oxidation or other impurities possibly added during heating the alloys in an atmosphere of nitrogen rather than the equilibrium vapour, i.e., mostly Sb. Moreover estimations of the compositions from the d values obtained from the back reflection region of the X-ray photographs, as in the present investigation, are much more accurate.

Lattice constants. The x-ray powder photographs of ϵ' phase were indexed by Broderick and Ehret (1931), and these were utilised to identify the reflections of the ϵ' phase in the present investigation. The reflections used for calculation of lattice constants were 004, 042 and 223. The lattice constants for the sample with 27.0 weight per cent Sb (Ag_3Sb)

Table 3

Table showing the compositions and lattice constants of the runs in ε phase.

Composition Wt. % Sb	Temp. C	Annealing time, days	Å Cell dimensions a	c
14.3	400	10	2.948	4.7844
14.97	400	10	2.946	4.8117
15.97	400	10	2.960	4.7896
16.86	400	10	2.967	4.7908
17.99	400	10	2.9752	4.7916

Table 4

Table showing the composition and cell dimension of the runs in the ε′ phase.

Composition Wt. % Sb	Temp. C	Annealing time, days	Lattice constants a	b	c
22.03	400	10	2.9876	5.1746	4.8068
22.99	400	10	3.0166	5.1746	4.8065
24.93	400	10	3.0088	5.190	4.822
27.00	400	10	3.0161	5.192	4.7961

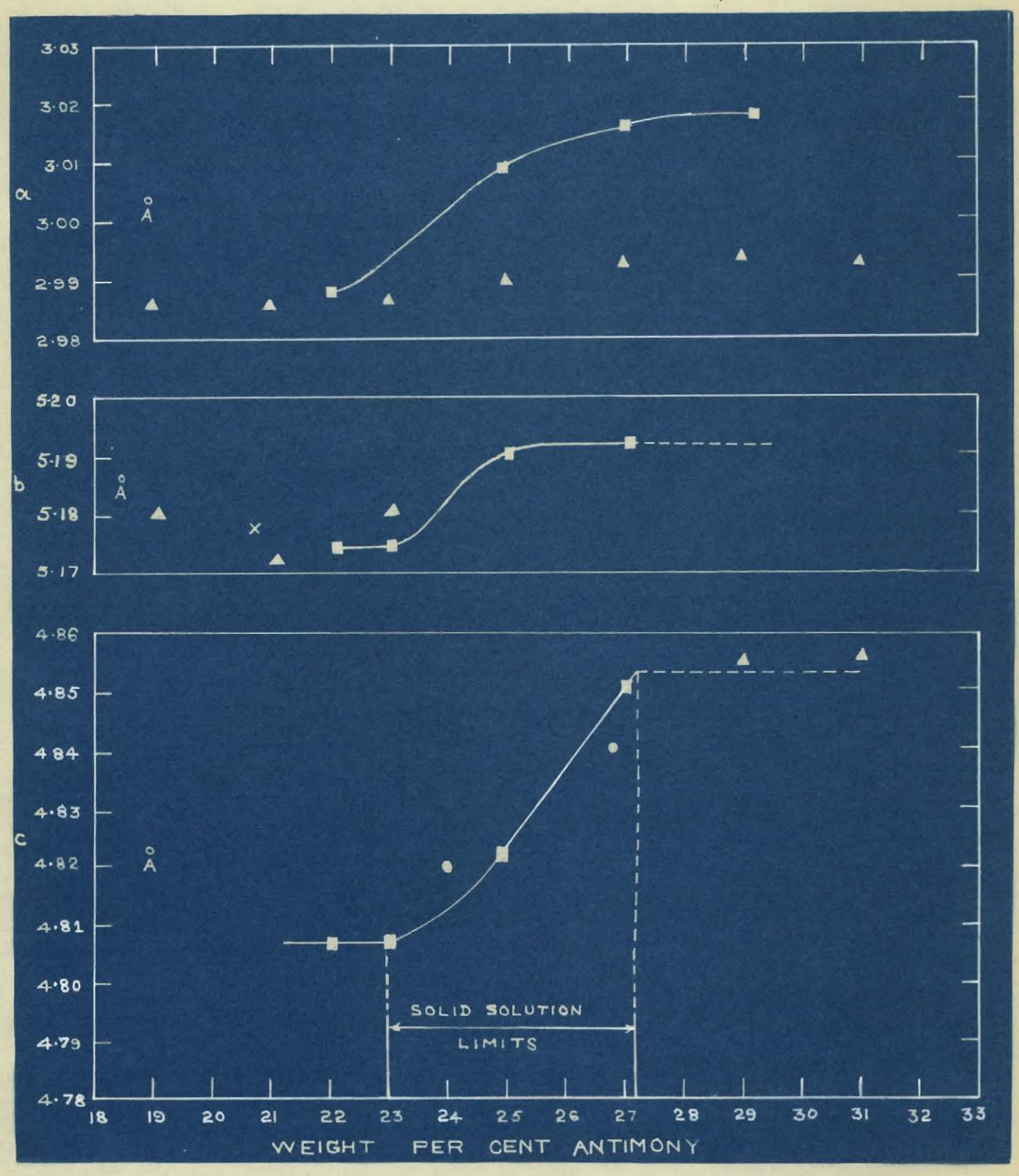

Figure 9: Lattice dimensions versus composition curve for the ε′ phase in the system Ag-Sb. Solid solution limits are taken from Figure 8.

× Broderick and Ehret.

○ Westgren, Hagg and Ericksson.

△ Weibke & Efinger.

□ Present investigation.

are a=3.0161, b=5.192, and c=4.7961 (see table 4).

The composition versus lattice constant curves show good linearity (see figure 9). This is a further suggestion that equilibrium was not attained by the previous investigators. Although not invariably the case, a straight line relation has usually been found for equilibrium solid solutions in other systems, see for example, Skinner, Barton and Kullerud (1959), Roseboom (1962), and Clark and Kullerud (in press).

Chapter 5

The Quasi Binary System Ag_2S - Sb_2S_3

An attempt was made to determine the solid solution boundaries of the minerals pyrargyrite and miargyrite at 400°C. Although no conclusive results were obtained, they seem to indicate extremely narrow solid solution fields.

Pyrargyrite. Five runs with varying compositions were prepared from the end members Ag_2S and Sb_2S_3, homogenized at 750°C for a period of 12 hours, annealed for a period of 15 days at 400°C, and quenched to room temperature. The products were then studied both microscopically and by X-ray methods. The results are summarized in table 5.

Table 5

Table showing the results of the polished section study of the runs containing pyrargyrite.

Sb_2S_3 (Wt. %)	Phases present
28.89	Ag_2S and pyrargyrite
30.37	Ag_2S and pyrargyrite
31.39	Pyrargyrite
32.2	Pyrargyrite and miargyrite ?
33.4	Pyrargyrite and miargyrite ?

It was not possible to study the solid solution limits by X-ray methods because of the complexity of the X-ray powder

pattern. Both Ag_2S (the cubic form stable at 400°C inverts to monoclinic during cooling) and pyrargyrite give complex X-ray diffraction patterns which are superimposed when present together.

The limits of solid solution could not be accurately determined as a result of the small number of runs prepared, as well as the difficulty of identification of small quantities of pyrargyrite in miargyrite or miargyrite in pyrargyrite under the microscope.

Only one sample, with a composition of 31.39 weight per cent Sb_2S_3 contained pure pyrargyrite (Ideal $3Ag_2S.Sb_2S_3$ contains 31.4 weight per cent Sb_2S_3). It is inferred that the solid solution limits are very narrow, probably between 31.0 and 32.0 weight per cent Sb_2S_3. Synthetic pyrargyrite prepared at 400°C showed no change in X-ray pattern after heating at 300°C.

Miargyrite. Six runs with varying compositions in the composition range 56.84 to 59.7 weight per cent Sb_2S_3 were prepared from the end members Ag_2S and Sb_2S_3. These were annealed at 400°C for a period of 15 days and quenched to room temperature. The products were studied both under the microscope and by X-ray methods. The results are summarized in table 6.

In identifying the different phases present, the same difficulties as in the previous case were encountered in the first two samples. It was found difficult to identify small

quantities of either pyrargyrite in miargyrite or miargyrite in pyrargyrite under the microscope. The results of the first two samples were obtained from X-ray study. They both contain miargyrite and pyrargyrite. Only the run with a composition of 57.93 weight per cent Sb_2S_3 contained pure miargyrite. (Ideal $Ag_2S.Sb_2S_3$ contains 58.0 weight per cent Sb_2S_3). The other runs contained miargyrite and stibnite. From this it was inferred that the limits of solid solution of miargyrite at 400°C are between 57.8 and 58.44 weight per cent Sb_2S_3. The limits are probably much narrower than these.

Table 6

Table showing the results of the polished section study of the runs containing miargyrite.

Sb_2S_3 (wt. %)	phases present
57.28	Pyrargyrite and miargyrite
57.8	Pyrargyrite and miargyrite
57.93	Miargyrite
58.44	Miargyrite and stibnite
59.115	Miargyrite and stibnite
59.7	Miargyrite and stibnite

A sample of pure miargyrite (57.93 weight per cent Sb_2S_3) was observed to have a cubic pattern in the X-ray diffraction photographs. The same sample after annealing for a period of 5 days at 300°C, gave a complex monoclinic X-ray powder pattern. The transition reported at 380°C (Jensen 1947) is evidently not rapid.

Chapter 6

Phase Relations in the System Ag - Sb - S at 400°C

In order to establish the tie lines bounding the equilibrium ternary assemblages, seven samples were prepared from the elements, melted and homogenized at 750°C for a period of from 6 to 12 hours, annealed at 400°C for a period of 16 to 20 days, and quenched to room temperature. A portion of each sample was prepared for X-ray study and another portion was utilized for polished section study. Results are summarized in table 7. Only reflections from the back reflection region in the X-ray powder patterns were used for calculating the compositions of the ε and ε' phases present, making use of the previously determined composition versus d spacing curves.

Table 7

Table showing the composition and the phases present in the runs in the system Ag - Sb - S annealed at 400°C.

Run.	Composition Wt.% Ag	Sb	S	Annealing time, days	Phases present in the Ag-Sb-S system at 400°C
1	91.0	6.0	3.0	16	α , β Ag_2S and ε
2	83.9	6.95	9.15	16	β Ag_2S, ε and $3Ag_2S.Sb_2S_3$
3	75.02	19.03	5.95	16	ε , $3Ag_2S.Sb_2S_3$ and ε'
4	61.00	25.0	13.99	20	$3Ag_2S.Sb_2S_3$, ε' and α $Ag_2S.Sb_2S_3$
5	69.0	27.0	4.0	16	$3Ag_2S.Sb_2S_3$, ε' and α $Ag_2S.Sb_2S_3$
6	46.0	40.0	14.0	16	ε', α $Ag_2S.Sb_2S_3$ and Sb
7	20.0	59.7	20.3	16	α $Ag_2S.Sb_2S_3$, Sb and Sb_2S_3

Sample 1 (see figure 10 and table 7), indicated the presence of Ag_2S, α and ε phases. No exact percentages could be calculated from these patterns because of the interference of the complex X-ray powder diffraction patterns of Ag_2S (III)* with the other phases. The interference of the complex β Ag_2S lines might have been avoided through the use of a high temperature camera where the specimen was kept above 178°C, the inversion temperature.

From sample 2 the tie line connecting the Sb-rich side of the ε phase to Ag_2S was obtained. The two-field region of ε+pyrargyrite was deduced from sample 3. This field was observed to be very narrow (between 17.0 and 17.7 weight per cent Sb), and this observation agrees with the results obtained by Barstad (1959).

Sample 3 indicates the presence of pyrargyrite, ε and ε' phases. The tie line connecting the ε' phase on the silver-rich side to pyrargyrite was also deduced from this sample with the aid of figure 8. The phase boundary of ε' phase on the silver-rich side agrees well with that obtained in the Ag-Sb binary system. Samples 4 and 5 were used to get the tie lines connecting the antimony-rich side of the ε' phase to pyrargyrite. The boundary of the narrow two-phase region between ε' and miargyrite was also obtained (see figure 10). The composition range of the ε' in this region is between 26.1 & 27.2 wt.%

---

* Ag_2S is cubic at the temperature of the run (β Ag_2S).

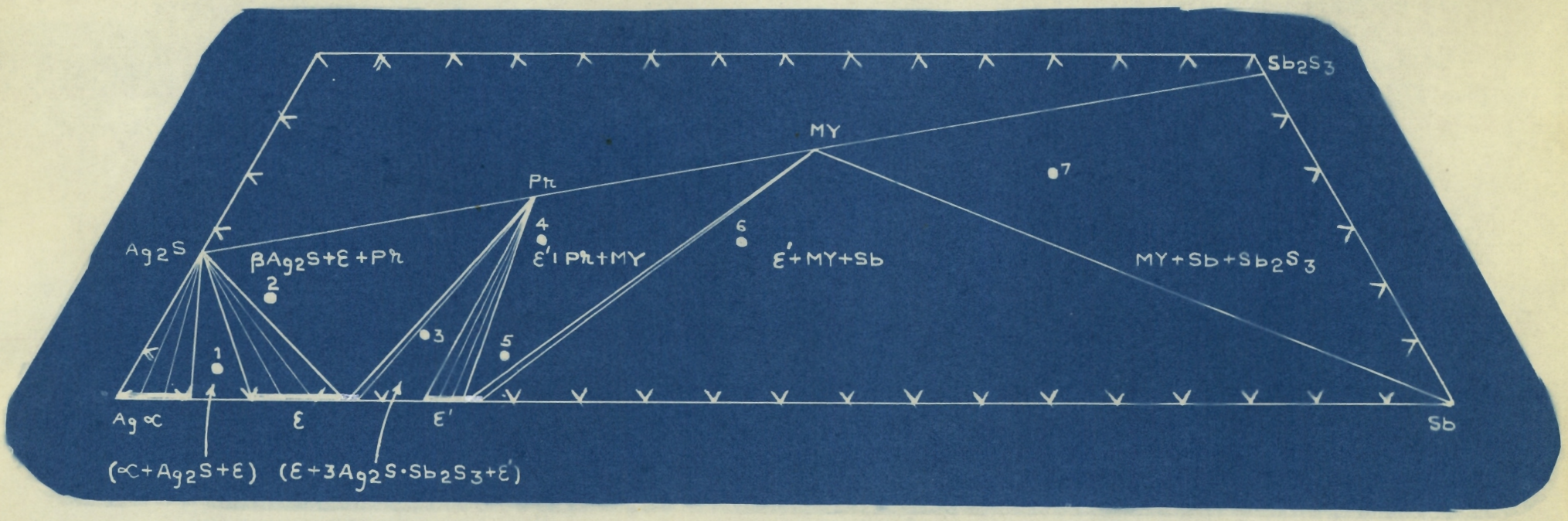

Figure 10: Isothermal section of the phase diagram of the system Ag-Sb-S at 400°C covering the region Ag-Sb-Ag_2S-Sb_2S_3.

per cent Sb. The composition of dyscrasite is approximately 27.1 weight per cent Sb, and this apparently falls in this region.

The phases present in samples 4 and 5 are ε', pyrargyrite and α $Ag_2S.Sb_2S_3$. The tie line connecting the Sb-rich end of the ε' phase to α $Ag_2S.Sb_2S_3$ was obtained from sample 6. The assemblage in sample 7 was Sb, ε' and α $Ag_2S.Sb_2S_3$. Thus the tie line was established between Sb and α $Ag_2S.Sb_2S_3$.

The results obtained from my work are in general agreement with those of Barsted (1959). Principal differences are, 1) phase assemblage boundaries are modified in accordance with the current changes in the Ag-Sb system, and 2) compositions of the ε and ε' phases coexisting in the three phase assemblages were actually determined rather than being inferred.

Phase Relations in the System Ag - Sb - S at 300°C

Ten samples whose compositions were in three-phase fields were prepared and annealed at 300°C for a period of 20-24 days.

The composition of the samples and the phases present are summarized in table 8 and figure 11.

The phases present in sample 8 are α , ε and β Ag_2S. Again the complex pattern of the β Ag_2S interfered with the accurate measurements of the reflections for α and ε . However, the phases present were easily identified. It is deduced that the tie lines from the whole α solid solution region are directed towards β Ag_2S.

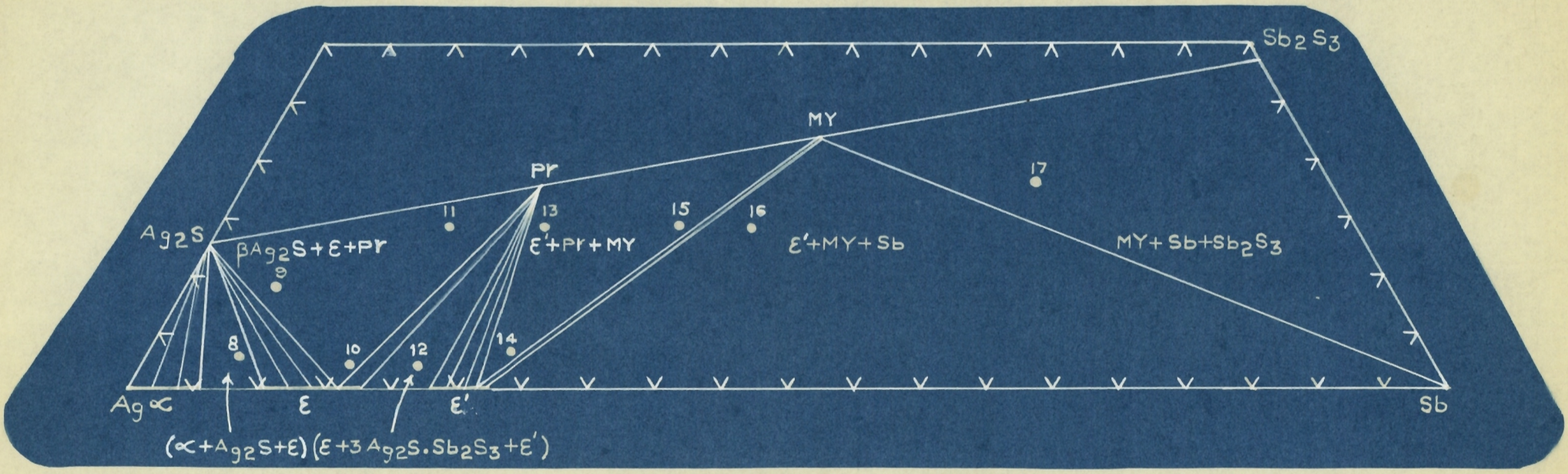

Figure 11: Isothermal section of the phase diagram of the system Ag-Sb-S at 300°C covering the region $Ag-Sb-Ag_2S-Sb_2S_3$.

The assemblage ε , β Ag_2S and $3Ag_2S.Sb_2S_3$ occurred in samples 9, 10 and 11. From samples 9 and 11 the tie lines connecting a portion of the ε phase solid solution field to β Ag_2S were obtained. On the ε solid solution a narrow portion is tied to $3Ag_2S.Sb_2S_3$ (Pr). This two-phase region now encompasses more of the ε solid solution field than the comparable assemblage at 400°C (see figure 10). In the present case it is between 15.9 and 17.7 weight per cent Sb.

Table 8

Table showing the composition and phases present in the runs in the system Ag - Sb - S annealed at 300°C.

Run	Composition wt. % Ag	Sb	S	Annealing time, days	Phases present in the Ag-Sb-S system at 300°C
8	90.07	6.9	3.03	24	α, β Ag_2S and ε
9	84.16	6.7	9.14	24	β Ag_2S, ε and $3Ag_2S.Sb_2S_3$
10	82.1	15.8	2.1	20	β Ag_2S, ε and $3Ag_2S.Sb_2S_3$
11	68.61	17.52	13.87	22	β Ag_2S, ε and $3Ag_2S.Sb_2S_3$
12	77.1	20.9	2.0	22	ε , $3Ag_2S.Sb_2S_3$ and ε'
13	61.1	24.85	14.05	22	$3Ag_2S.Sb_2S_3$, ε' and β $Ag_2S.Sb_2S_3$
14	69.2	27.6	3.2	20	$3Ag_2S.Sb_2S_3$, ε' and β $Ag_2S.Sb_2S_3$
15	50.85	35.0	14.15	20	$3Ag_2S.Sb_2S_3$, ε' and β $Ag_2S.Sb_2S_3$
16	45.58	40.42	14.0	22	ε', β $Ag_2S.Sb_2S_3$ and Sb
17	22.05	60.13	17.82	21	Sb, β $Ag_2S.Sb_2S_3$ and Sb_2S_3

The phases ε , $3Ag_2S.Sb_2S_3$ and ε' are present in sample 12.

Samples 13, 14 and 15 show the three phases ε' , $3Ag_2S.Sb_2S_3$ and β $Ag_2S.Sb_2S_3$ (my). The complex β $Ag_2S.Sb_2S_3$ reflections overlapped the lines of the other phases, and this created a problem for calculating the lattice constants. But the compositions of the phases in the Ag-Sb system were calculated using the lines in the back reflection region utilizing the composition versus d-spacing curves prepared for the Ag-Sb system (figures 5 and 8). Sample 16 showed the presence of the three phases ε' , β $Ag_2S.Sb_2S_3$ (my) and Sb. The composition of the ε' phase as measured from this sample coincides with the solid solution limit of ε' phase on the Sb-rich side in the phase diagram Ag-Sb at 300°C.

The solubility of sulphur in the phases α , ε and ε' in the Ag-Sb system seems to be insignificant as the phase boundaries of these phases, as obtained in this system, are almost identical with those in the Ag-Sb system.

The narrow two-phase region between ε' phase and β $Ag_2S.Sb_2S_3$ includes ε' compositions in the range 26.1 to 27.2 weight per cent Sb. This range is similar to that at 400°C.

Sample 17 showed the presence of the phase Sb_2S_3. It is inferred from these two samples (16 and 17) that the tie line from Sb is directed towards miargyrite (β $Ag_2S.Sb_2S_3$).

Partial solidus - liquidus relations along the pseudo-binary Ag_3Sb - $3Ag_2Sb.Sb_2S_3$ join.

It was observed that the samples 1 to 5 at 400°C (figure 10) and 8 to 14 at 300°C (figure 11) contained a globule of a metallic

silver-rich phase embedded in a more powdery material containing the other phases present. This formed an "onion" structure and the size of the globule was progressively reduced in more antimony-rich bulk compositions. From this the presence of a two-liquid field was suspected in this region. X-ray and microscope study of the samples revealed that the globule was the Ag-Sb-phase stable for the assemblage.

To test the two-liquid hypothesis a series of three samples falling within the two phase region of Ag_3Sb (dy) and $3Ag_2S.Sb_2S_3$, were prepared and studied on a modified differential thermal analysis apparatus. Finely-powdered galena was used as the inert sample. The results obtained are shown in figure 12. The melting point of $3Ag_2S.Sb_2S_3$ was taken from Jensen (1947).

The diagram shows a eutectic between 22 and 26 weight per cent $3Ag_2S.Sb_2S_3$. The solidus is at 458 $\pm$ 5°C throughout the region. The liquidus departs from the section on approaching the Ag_3Sb side of the pseudo-binary. Determinations in this area are beyond the scope of the present investigation and would be of little geological interest.

No evidence of a two-liquid field was found. This indicates that the tie lines in the figures 10 and 11 are directly connected, as determined, to the different phases without the interference of a two-liquid field in this region.

No extensive homogeneity ranges of the phases Sb_2S_3, Sb, $Ag_2S.Sb_2S_3$ and $3Ag_2S.Sb_2S_3$ were observed.

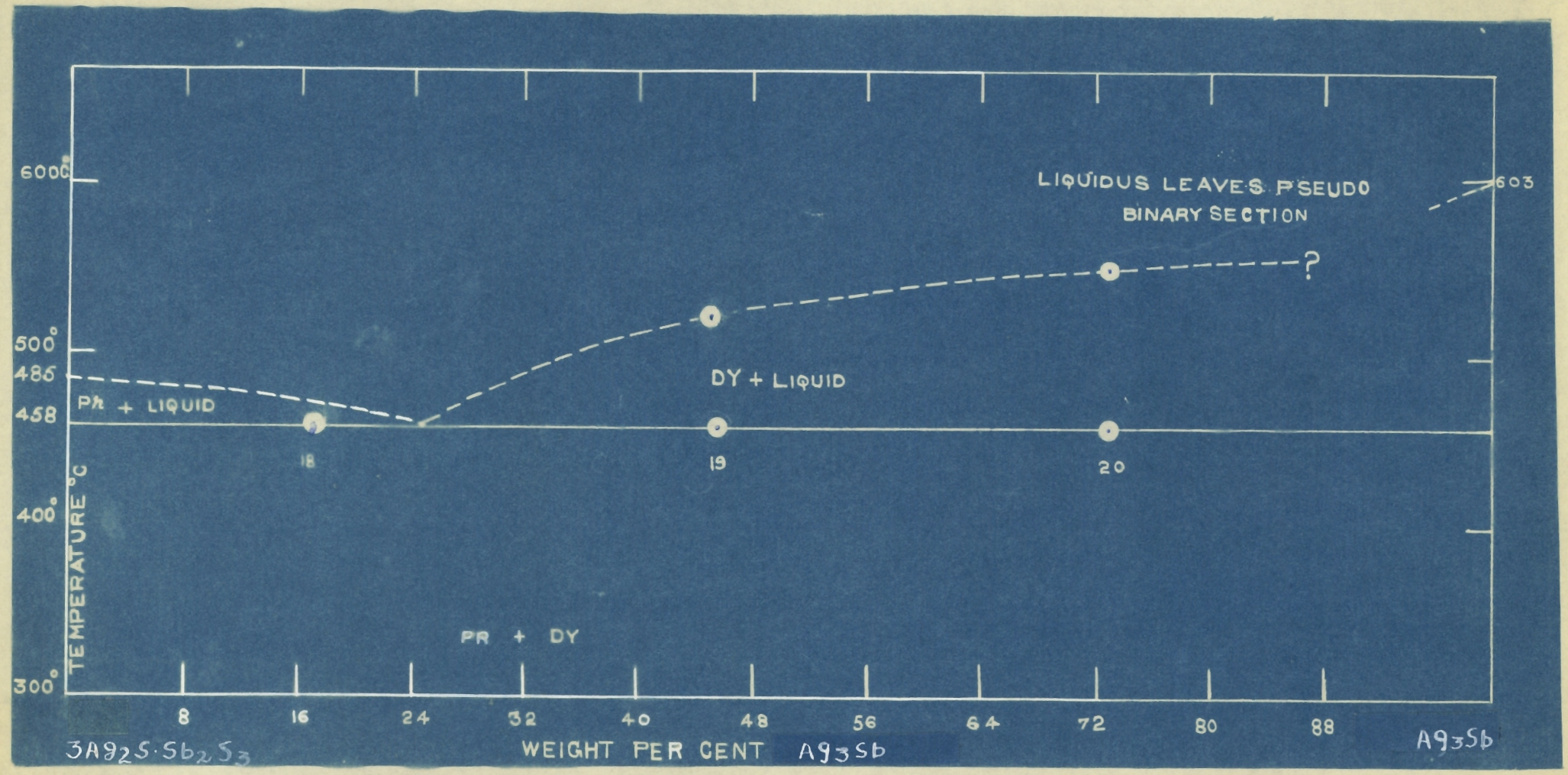

Figure 12: Partial solidus-liquidus relations along the pseudo-binary Ag_3Sb-$3Ag_2S.Sb_2S_3$ Join.

Two narrow two-phase regions are present, one extending from Sb-rich side of the ϵ solid solution field to $3Ag_2S.Sb_2S_3$, and the other extending from the ϵ' phase to $Ag_2S.Sb_2S_3$, in isothermal sections at both 400°C and 300°C. The two-phase region extending from the ϵ' phase in the isothermal section at 300°C is slightly wider. It is probable that with decreasing temperature this field might get wider.

Chapter 7

The Occurrence of Ag - Sb minerals

A crystalline mineral composed essentially of silver and antimony was known to Rome de l'Isle and to Werner in the eighteenth century. Early named antimonial silver this mineral received the name "dyscrasite" (Beudant, 1832) which has been applied to crystallized and massive materials composed of silver with varying proportions of antimony. Andreasberg in the Harz Mountains was one of the earliest known locations for dyscrasite. Most of the later investigations of this mineral were conducted on samples from this area.

The existing analyses of materials referred to as "dyscrasite" (Doelter, 1926) range from about Ag 73, Sb 27 weight per cent, corresponding to Ag_3Sb, to about Ag 84, Sb 16 per cent, giving Ag_6Sb.

Dyscrasite. Machatschki (1928) investigated a sample of dyscrasite from Andreasberg and concluded that the mineral has a general composition Ag_3Sb. Peacock (1940) studied a crystal of dyscrasite from Andreasberg and came to the same conclusions. The lattice constants are a=2.996, b=5.235, c=4.830; Z=1. Most of the workers in this field recognized only one compound, Ag_3Sb, as a natural mineral, and grouped the rest of the silver antimony compounds either under antimonial silver or were thought to be a eutectic intergrowth of silver and an antimonide of silver. Schwartz (1928) obtained etch relations from a specimen such as to indicate that the lamellae consisted of α solid

solution phase and the matrix of Ag_3Sb (ε' phase).

The silver-cobalt ores at Cobalt, Ontario, include distinctive exsolution intergrowths of these Ag-Sb minerals. These consist generally of blades or lamellae of a mineral regarded as dyscrasite (Ag_3Sb, ε' phase) oriented in the (111) direction of a second mineral, which is generally regarded as antimonial silver (α phase) (Peacock, 1940).

The ε phase. The ε phase is not so prevalent but has been found at Andreasberg in the Harz Mountains, where it has been confused with dyscrasite (Peacock, 1940). Burrows (1921) analyzed a sample from La Rose mine, Cobalt, Ontario, which Miller termed "dyscrasite" and gave the general formula Ag_6Sb. Later Walker (1921) microscopically examined specimens from the Timiskaming and Kerr Lake Mines, and found a mixture of dyscrasite and native silver in fine intergrowth. All of these workers, however, interpreted their observations in the light of an earlier version of the Ag-Sb equilibrium diagram. These earlier diagrams showed only the α and ε' phases, and failed to indicate the ε phase (Weibke and Efinger, 1946). This probably is the reason for not listing the compound Ag_6Sb, which falls in the ε phase, as a natural mineral.

Prior to the discovery of the ε phase in the synthetic system Ag-Sb (Weibke and Efinger, 1940) Carpenter and Fisher (1932), in studying a specimen from Cobalt, Ontario, concluded that if Ag_3Sb was present in the natural intergrowth, it formed the matrix, and the lamellae consisted of the α phase solid

solution. Since this was inconsistent with the equilibrium diagram available to them, they suspected that the diagram was wrong. Edwards (1954) re-interpreted their results in the light of the new diagram as either (a) the lamellae consist of dyscrasite (ε' phase) in a matrix of ε phase (Ag_6Sb), or (b) the lamellae consist of α phase in a matrix of ε phase. Ramdhor (1960) identified ε phase in polished sections from Cobalt, Ontario, and called it "allargentum". He did not give any X-ray or chemical analysis data to verify its identity. He describes the mineral as having properties between those of dyscrasite and antimonial silver. Its reflectivity is slightly more than dyscrasite and its hardness nearly equal to that of dyscrasite. In his photograph of the polished section, the three phases α , ε , and ε' were present, which, in view of the phase rule, is an impossible assemblage. This could happen only when one of the phases is metastable.

Re-interpretation of the chemical analyses of Ag-Sb minerals.

A study of the analyses of Ag-Sb minerals from different localities (Walker, 1921, and Doelter, 1926) in the light of the new equilibrium diagram, brings out certain interesting features (see table 9). It will be noticed that all the analyses fall into three distinct groups. In the first group the antimony content varies from 5.89 to 6.78 weight per cent Sb, in the second from 11.18 to 16.17 weight per cent Sb, and in the third group from 22.00 to 27.88 weight per cent Sb. The limits of these three groups correspond to a remarkable extent to the limits of the three solid solution fields namely,

Table 9

Table showing the chemical compositions of Ag-Sb minerals, localities and the probable phase to which each belongs. Analyses from Walker (1921), and Doelter (1926).

	Wt. % Ag.	Sb.	Total	Phase		Locality
	84.00	16.0	100	ε		Wenzelsgang, Black Forest
	84.7	15.0	99.7	ε		Andreasberg, Harz Mountains
	83.85	15.81	99.66	ε		Wenzelsgang
	83.9	16.17	100.07	ε		Andreasberg
	76.0	24.0	100	ε'		Wenzelsgang
	75.25	24.75	100	ε'		Andreasberg
	78.00	22.0	100	ε + ε'		"
	77.0	23.0	100	ε'		"
	72.34	27.66	100	ε'		"
	72.36	27.64	100	ε'		"
	72.62	27.88	100	ε'		"
	72.42	25.58	100	ε'		"
	74.67	25.33	100	ε'		"
	75.28	24.72	100	ε'		"
	74.9	24.75	99.65	ε'		"
	75.86	24.3	100.16	ε'		"
	76.83	23.35	100.18	ε'		"
	74.41	25.52	99.93	ε'		"
	75.39	24.63	100.02	ε'		"
	75.13	24.94	100.7	ε'		"
	75.38	24.12	99.5	ε'		"
	71.52	27.2	98.72	ε'		Wenzlesgang
	76.65	23.06	99.71	ε'		"
	76.92	23.92	100	ε'		Carrizio in Capiapo', Chile
	77.72	22.28	100	ε + ε'	?	"
	77.12	22.1	99.22	ε + ε'	?	"
	77.58	11.18	99.31	ε		Silver Islet Mine, L.Superior
x	92.19	6.78	99.42	α		Temiskaming Mine, Cobalt,Ont.
x	85.47	12.99	99.58	ε		Kerr Lake Mine " "
x	93.63	5.89	99.85	α		Buffalo Mine " "
x	92.6	6.59	99.75	α		Cobalt, Ontario
x	83.9	15.6	99.5	ε		La Rose Mine " "

x Walker (1921)

α , ε and ε' phases in the system Ag-Sb. From this the natural inference seems to be that these compounds are distinct minerals, and only the lack of a correct phase diagram led the previous workers to divide the silver-antimony minerals into only two groups namely, antimonial silver (α phase) and dyscrasite (ε' phase).

A specimen from Cobalt, Ontario (No. 221 - M1, McGill collection), has been examined, and the two phases, α and ε identified. A small portion of the laboratory specimen was utilized for X-ray study. Two portions of the filings were annealed for 12 hours at 300 and 415°C, respectively. The X-ray powder patterns of both the samples are similar. The material after annealing at these temperatures, has attained homogeneity, and gave the powder pattern of ε phase without extra reflections. The composition of this homogeneous phase, as determined with the help of the d value versus composition curve of the ε phase (see figure 5), is 13.9 weight per cent antimony. The implication is that the mineral originally crystallized as a homogeneous phase in the solid solution field, and as the deposit cooled, antimonial silver was exsolved.

A small piece of the original specimen was examined under the reflecting microscope. Two phases were observed in the sample, antimonial silver and the ε phase. Under the microscope the mineral exhibits extensive exsolution features. Antimonial silver occurs as irregular, rounded patches 0.20 mm. in size, embedded in a matrix of ε phase. A rough estimate

of the quantities of both the phases indicated that approximately 70 per cent of the material consists of ε phase. The patches of antimonial silver exhibit a feathery type of exsolution structure where α and ε are in almost equal proportions. In this case the two phases exhibit a fine lamellar intergrowth, the size of the lamella being 0.05 mm.

Under the microscope the ε phase is light greyish in colour and shows a slight anisotropism. It is slightly harder than antimonial silver (see Plate 1).

The extensive exsolution indicates a relatively high temperature of formation and considerably shallower slopes for the solvus curves of both α and ε phases than are indicated by previous experimental work (see figure 6).

X-ray study of the natural mineral without annealing, clearly shows the presence of antimonial silver (see Plate 3). Lines representing the ε phase are also present (see table 10). Peacock (1940), in studying a similar mineral, reported that the X-ray powder photographs showed weak reflections corresponding to the strongest lines of pure dyscrasite. But in my studies of the synthetic dyscrasite (ε' phase) and ε phase, the strongest reflections in both these phases are similar enough to be uncertain due to spacing variations with solid solution changes (see table 10). The only reliable and distinctive reflections occur at higher 2θ angles, and these lines are always weak.

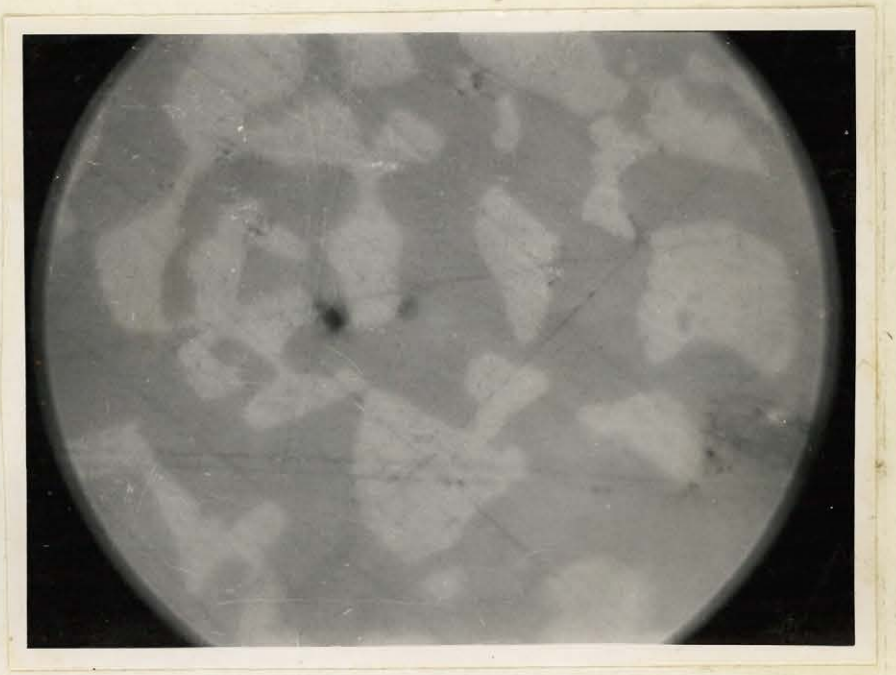

Plate 1.

Plate 2.

Table 10

Table comparing the X-ray powder diffraction patterns of α, ε, ε', and naturally occurring mixture of antimonial silver and phase from Cobalt, Ontario (No.221 - M1, McGill collection).

Antimonial Silver[1] (α phase)			Allargentum[2] (ε phase)			Dyscrasite[3] (ε' phase)			No. 221 - M1		
d, Å	hkl	I	d, Å	hkl	I	d, Å	hkl	I	d, Å	I	Phase
			2.5446	100	MS	2.61	020 110	MS	2.553	S	ε
2.37	111	VVS	2.3848	002	S	2.42	002	S	2.3781	VVS	ε
			2.2485	101	VVS	2.29	021 111	VVS	2.2121	VVS	?
2.059	002	S							2.0561	MS	α
			1.743	102	MS	1.771	022 112	MS	1.7473	MS	ε
			1.4731	110	MS	1.506	130 230	MS	1.4775	MS	ε
1.455	022	MS							1.4513	MS	α
			1.3525	103	MS	1.37	023 113	S	1.3561	MS	ε
			1.2763		VVW	1.278	132 202	MS			
			1.2556		VS	1.258	041 221	MS	1.2587	MS	?
1.241	113	MS	1.2338	201	? VW				1.2388	MS	ε
1.188	222	W				1.207	004	W	1.1980	W	α
						1.148	042 222	W			
			1.127	202	W						
			0.9976	023	VW	1.096	024 114	MS	0.9968	VVW	ε
			0.9654			0.964	151 241 311	W			
0.946	133	MS	0.9465	211	? VVW	0.942	134 204	MS	0.9427	VVW	?

1. From Berry and Thompson (1962). Natural material from Cobalt, Ontario.
2. Present investigation 14.97 Wt.% Sb.
3. From Berry and Thompson (1962). Natural material from Andreasberg.

VVS: Very very strong; VS: Very strong; S: Strong; MS: Medium strong. VVW: Very very weak; VW: Very weak; W: Weak.

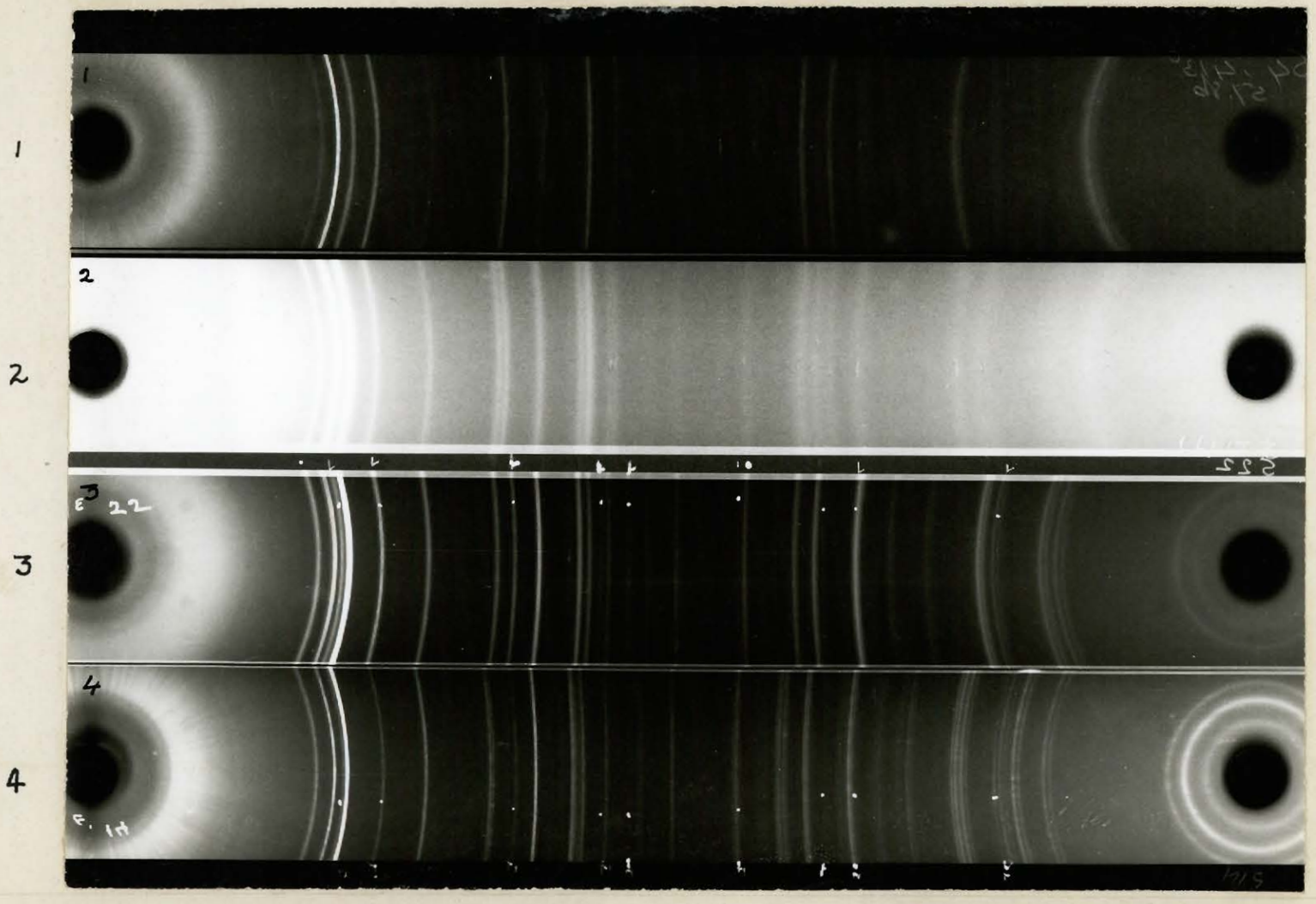

PLATE 3.

In the present case, the similarity of the reflections of the ε phase leaves no doubt as to the presence of ε phase in the sample under investigation (see table 10).

Conclusions

The phase boundaries as determined by previous workers are slightly different from the boundaries here determined. One reason for this is probably that the runs prepared by the previous workers were not in equilibrium due to a shorter annealing time. The lattice constants versus composition curves, as I have determined them, show marked linearity with composition. The determinations of previous workers show considerable scatter.

The ε phase boundary on the Sb-rich side shows a slight inclination. It is 17.7 weight per cent Sb at 300°C and 17.75 weight per cent Sb at 400°C. Above 450°C the amount of antimony taken in solid solution increases relatively rapidly to 18.2 weight per cent Sb at 500°C.

The boundary of the ε' phase on the Ag-rich side is 22.5 weight per cent Sb at 500°C and 22.9 weight per cent Sb at 450, 400, 350 and 300°C. The Sb saturation boundary is 27.2 weight per cent Sb at 500, 450, 400 and 350°C and 26.9 weight per cent Sb at 300°C.

No inversion of ε' to ε'' at about 440 and 449°C, as has been indicated by Weibke and Efinger (1940), was observed.

The occurrence of ε phase in the mineral from Cobalt, Ontario was proved by X-ray studies. This phase occurs along with antimonial silver (α phase). Both the

phases contain exsolutions of the other as shown under the microscope.

Experiments to determine the solid solution limits of pyrargyrite and miargyrite showed that the homogeneity ranges in both the cases are very narrow. It is probably less than one weight per cent Sb_2S_3 at 400°C in the case of pyrargyrite. Pyrargyrite synthesized at 400°C showed no change in X-ray pattern after heating at 300°C.

The limit of solid solution of miargyrite at 400°C is less than 0.6 weight per cent Sb_2S_3. The high temperature form of miargyrite could be preserved at room temperature by rapid cooling. The transition reported at 380°C is evidently not rapid.

No extensive homogeneity ranges of the phases Sb_2S_3, Sb, $Ag_2S.Sb_2S_3$ and $3Ag_2S.Sb_2S_3$ were observed. The solubility of sulphur in the phases α, ε and ε' in the Ag-Sb system seems to be insignificant as the boundaries of the ternary two phase assemblages are almost identical with the solid solution limits in the Ag-Sb system.

Two narrow two-phase regions, one extending from Sb-rich side of the ε solid solution field to $3Ag_2S.Sb_2S_3$ and the other extending from the ε' phase to $Ag_2S.Sb_2S_3$ were observed in isothermal sections at both 400 and 300°C. The two-phase region $\varepsilon' - Ag_2S.Sb_2S_3$ is wider at 300°C than at 400°C and possibly may be still wider at lower temperature.

It is also observed that the tie lines in both the isothermal sections connect directly the ternary and Ag-Sb binary phases without the interference of a two-liquid field in this region.

References

1) Azàroff, L.V. and Buerger, M.J. (1958). The powder method in X-ray crystallography, McGraw-Hill Book Company.

2) Barstad, J. (1958). Phase relations in the system Ag-Sb-S at 400°C, Acta.Chem.Scandinavica, 13, No.8.

3) Berry, L.G. and Thompson, R.M. (1962). X-ray powder data for ore minerals, The Peacock Atlas, Geol.Soc. of America, Memoir 85.

4) Beudant, F.S. (1832). Traité élémantaire de Minéralogie, 8Vo, Paris, Second edition, Vol.2.

5) Bissett, C.C. (1914). J.Chem.Soc., 105, 1223-1228.

6) Broderick, S.J. and Ehret, W.J. (1931). An X-ray study of the alloys of silver with bismuth, antimony and arsenic, Part 1, J.Phys.Chem., 35, 2627-2636.

7) Burrous, A.A. (1921). Gowganda and other silver areas, Ontario Dept. of Mines, Vol.30, Pt.3.

8) Carpenter, H.C.H. and Fisher, M.S. (1932). A metallographic investigation of native silver, Trans. Inst. Min. Met., London, 41, 382-403.

9) Clark, L.A. and Kullerud, G. Phase relations in the sulphur-rich portion of the Fe-Ni-S system (in press.)

10) Clark, L.A. (1959). Phase relations in the Fe-As-S system, Ph.D. Thesis, Dept. of Geol.Sci., McGill University.

11) Doelter, C. (1926). Handbuch der Mineralchemie, Vol.4, Part 1, page 234, Dresden and Leipzig.

12) Edwards, A.B. (1954). The Texture of the ore minerals and their significance, Melbourne, Australian Inst. of Min. Met. (Ine.), 60-61.

13) Friedrich, K. and Leroux, A. (1906). Metallurgie, 3, 361-367.

14) Frueh, A.J. Jr. (1958). The crystallography of silver sulphide, Ag_2S, Akad.Verlag., M.B.H., Frankfurt Am Main.

15) Gaudin, A.M. and McGlashan, D.W. (1938). Sulphide silver minerals - A contribution to their pyrosynthesis and to their identification by selective iridescent filming, Econ. Geol., 31, 143.

16) Gottfried, C. (1927). Uber die Struktur des Antimonits, Z. Krist., 65, 428-434.

17) Graham, A.R. (1951). Matildite, aramayoite and miargyrite, Am. Mineralogist, 36, 436.

18) Hansen, M. and Anderko, K. (1958). Constitution of Binary alloys, Second edition, McGraw-Hill.

19) Harker, D. (1936). The Application of the Three-Dimensioned Patterson Method and the Crystal structure of Proustite, Ag_3ASS_3 and pyrargyrite, Ag_3SbS_3, J.Chem.Phys., 4, 381.

20) Heycock, C.T. and Neville, F.H. (1897). Phil. Trans. Roy. Soc., London, A 189, 52.

21) Hofmann, W. (1933). Die Struktur der Minerale der Antimonitgruppe, Z. Krist., 86, 225-245.

22) Jaeger, F.M. (1911-1912). Akad. Amsterdam Verslag, 20, 498.

23) Jaeger, F.M. and Van Klooster, H.S. (1912). Z. anorg. U. allgem. Chem., 78, 245.

24) Jensen, E. (1947). The system silver sulphide - Antimony trisulphide, Avhandl. Norske Videnskaps - Akad. Oslo, 1. Mat. Naturv. Klasse, No.2, page 23.

25) Kerr, P.F., Kulp, J.L. and Hamilton, P.K. (1949). Differential thermal analysis of reference clay mineral specimens, Reference Clay Minerals, A.P.I., Research project 49.

26) Kracek, F.C. (1946). Phase relations in the system sulphur - silver and the transition in the silver sulphide, Trans. Am. Geophys. Union, 27, 364-374.

27) Machatschkki, F. (1928). About the crystal structure of the flakey dyscrasite of Andreasberg (Harz) and the synthetic Ag_3Sb alloy system, Ztschr. Kristallogr. Mineral., 67, 169.

28) Olie, J. and Kruyt, H.R. (1911-1912). Akad. Amsterdam Verslag, 20, 69.

29) Peacock, M.A. (1940). "On dyscrasite and antimonial Silver", Univ. Toronto Stud., Geol. Ser., 44, 31.

30) Pelabon, H. (1906). Compt. Rend., 143, 294-296; Ann. Chim. et phys., (1909) 17, 526-566.

31) Petrenko, G.I. (1906). Z. anorg. Chem., 50, 133.

32) Puschin, N. (1907). Jour. russ. phys. chem. ges., 39, 528; C.1907, 11, 3028.

33) Ramdohr, P. (1960). Die Erzmineralien und ihre Verwarchsungern, Akademic Verslag, Berlin, 3rd edition, page 381.

34) Roseboom, E.H. Jr. (1962). Skutterudites (Co, Ni, Fe) As_{3-x}; Composition and cell dimensions, American Mineralogist, Vol.47, 310-327.

35) Schenck, R., Hoffmann, I., Knapper, W. and Vogler, H. (1939). Gleichgewichtsstudien Uber erzbildende Sulfide. 1, Z. anorg. U. allgem. Chem., 240, 173.

36) Schwartz, C. (1928). Am. Min., 13, 495.

37) Skinner, B.J., Barton, P.B. Jr. and Kullerud, G. (1959). Effect of FeS on the unit cell edge of sphalerite - A revision, Econ. Geol., 54, 1040-1046.

38) Swanson, H. and Taige. (1953). Standard X-ray diffraction powder patterns, NBL circular Vol.1, 539.

39) Urazov, G.G. (1915). J. Inst. Metals, 16, 234. (Abstract).

40) Walker, T.L. (1921). Contribution to Canadian Mineralogy, Univ. of Toronto Studies, Geol. Ser. No.12, page 20-22.

41) Weibke, F. and Efinger, I. (1940). Der Aufball der Legierungen des systems Silver-Antimon, Z. Elektrochem., 46, 52-60.

42) Weil, R. and Hocart, R. (1953). Compt. rend. congres soc. savantes, Toulouse, Sect. Sci., 183.

43) Westgren, A., Hagg, G. and Eriksson, S. (1929). Ronlgenanalyse der system Kupfer-Antimon und Silber-Antimon, Z. Physik. chem., 34, 461-468.

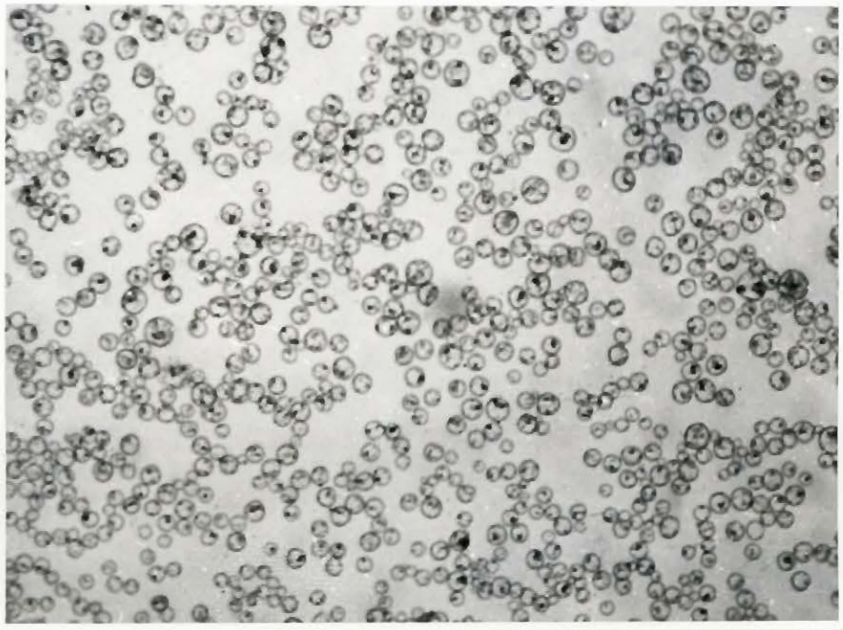

Fig. 2

Collodion-membrane microcapsules, containing hemolysate, in aqueous suspension. Mean diameter 18μ: magnification 60X. Note presence of precipitated protein in internal phase. The microcapsules in the original suspension had a yellowish-brown cast.

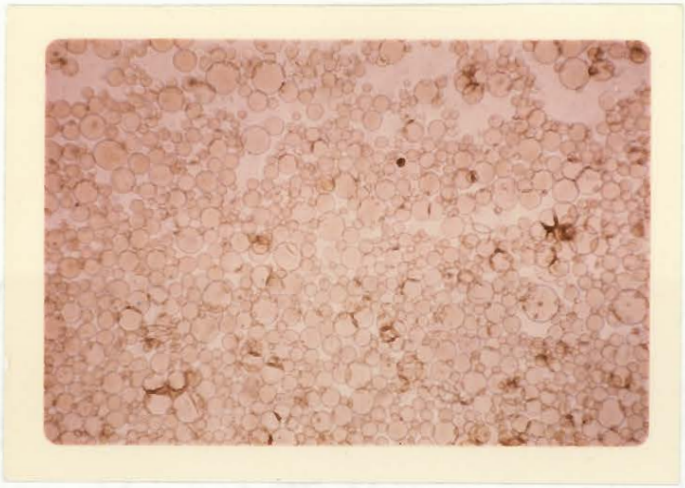

(A)

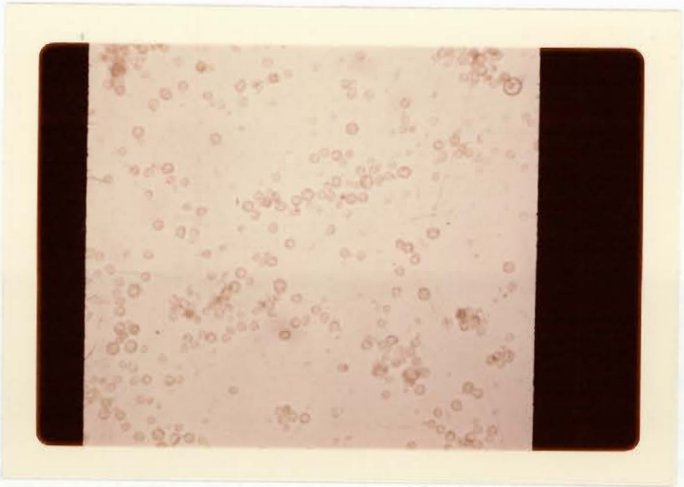

(B)

Fig. 3

(A) Nylon-membrane microcapsules, containing hemolysate, in aqueous suspension. Mean diameter 27 μ: magnification 60X. The darker patches in the microphotograph are areas where microcapsules are superimposed on one another.
(B) Smaller microcapsules of similar composition. Mean diameter 5 μ: magnification 250X.

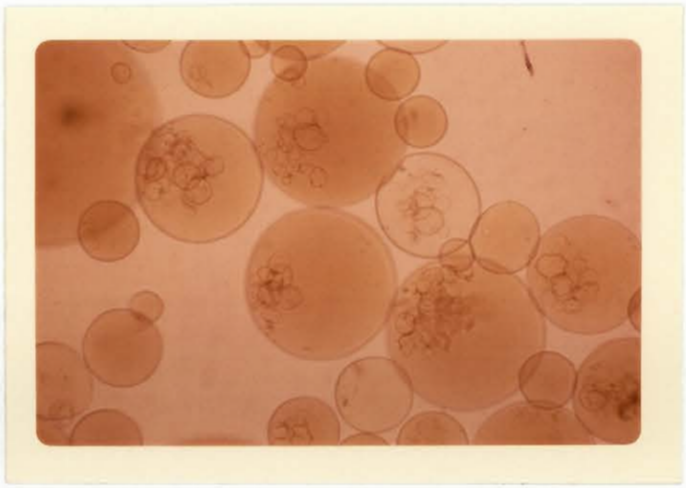

Fig. 13

Nylon microcapsules enclosing smaller Nylon microcapsules.
Magnification 60X.

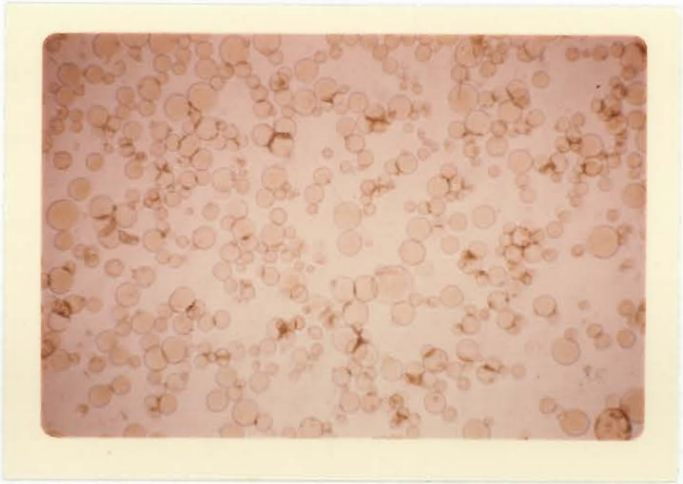

Fig. 6

Sulphonated-Nylon microcapsules containing hemolysate in aqueous suspension. Mean diameter 27 μ: magnification 60X.

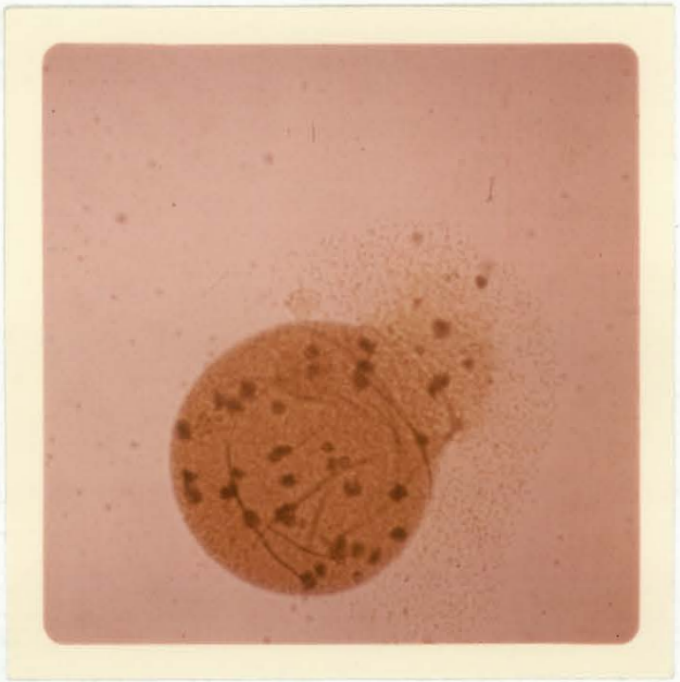

Fig. 14

Above Human erythrocytes enclosed within a large (500 μ) microcapsule with membrane of cross-linked haemoglobin. The reddish tint of the enclosed material is due partly to haemoglobin in free solution and partly to erythrocytes above or below the focal plane. There has been some folding of the microcapsule membrane under the influence of gravity. Magnification 250X.

Below Similar microcapsule in saline. The membrane has been ruptured by pressing on the coverslip and the contained erythrocytes are escaping. The dark patches are erythrocyte clumps produced by the cross-linking process. Magnification 60X.

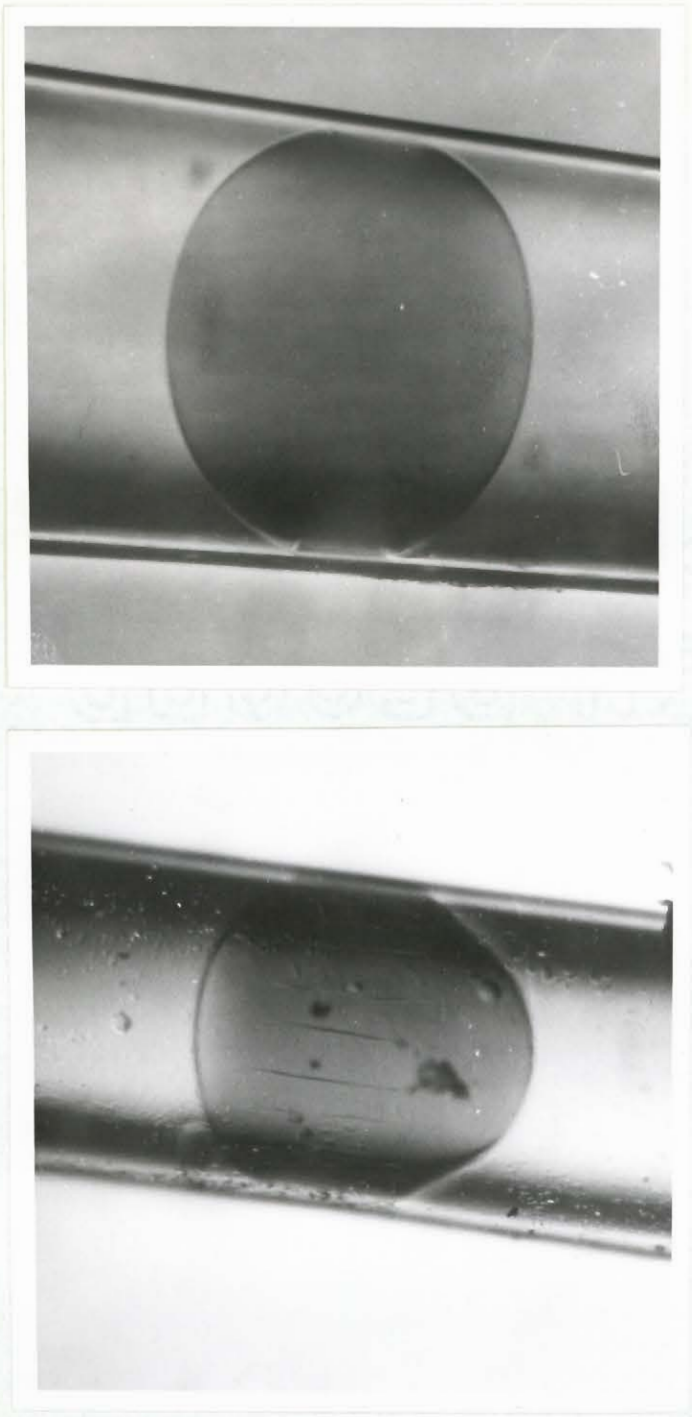

Fig. 15

Deformability of a Nylon microcapsule. The microcapsule, about 100 μ in diameter and suspended in saline, is moving from left to right along a tapering glass capillary. Above: (flow momentarily stopped) the microcapsule is just occluding the lumen of the capillary. Below: (flow again stopped) the microcapsule is in the narrowest part of the capillary and is subjected to a hydrostatic pressure gradient from left to right. Note flattening of upstream surface, bulging of downstream surface, longitudinal folding of membrane, and smaller volume of microcapsule as a result of filtration of fluid through downstream surface into capillary.

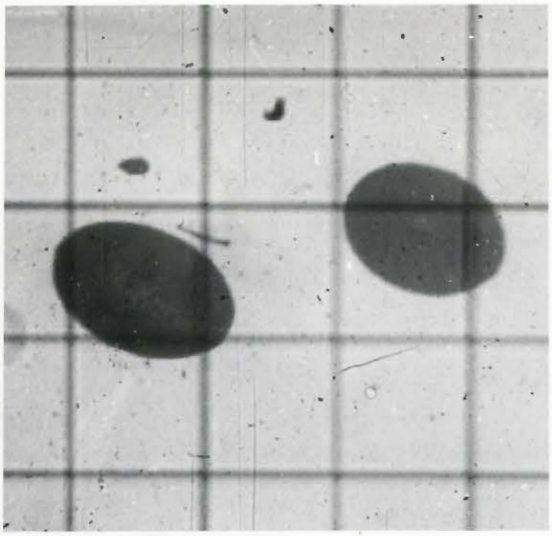

(a)

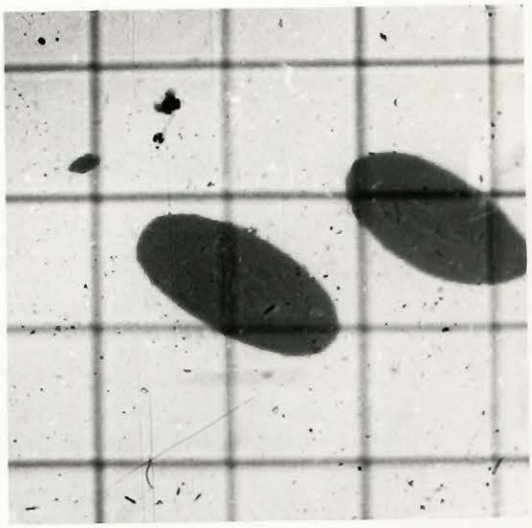

(b)

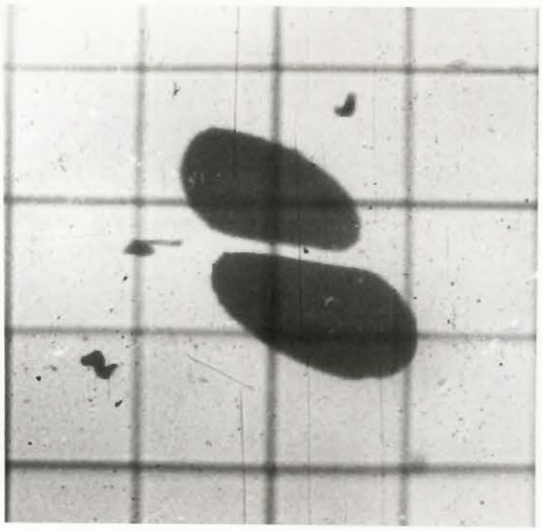

(c)

Figure 16

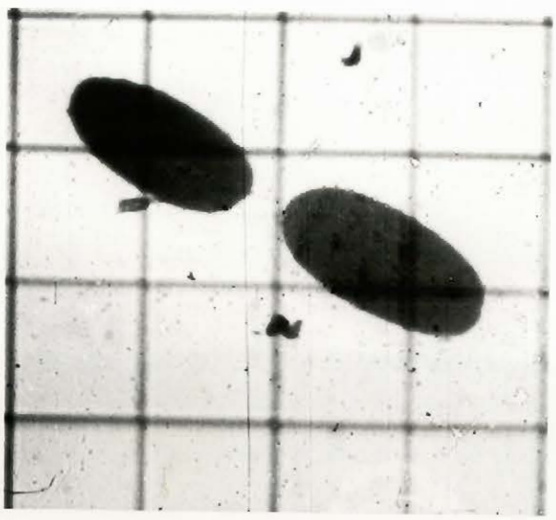

(d)

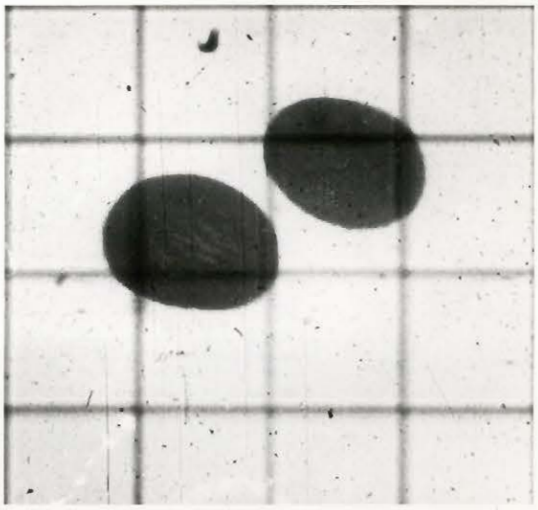

(e)

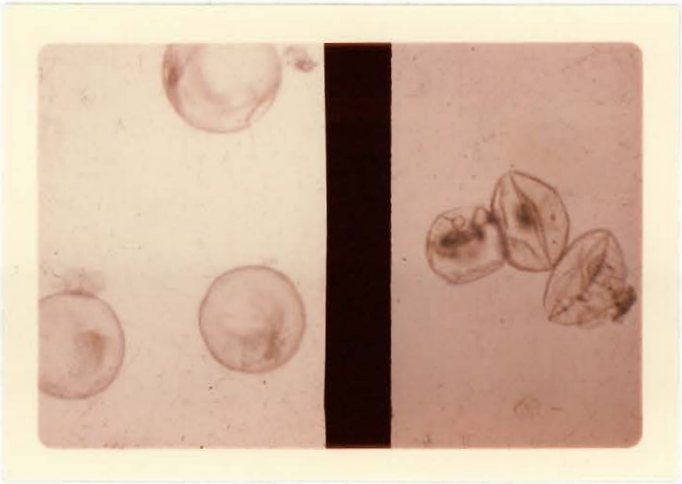

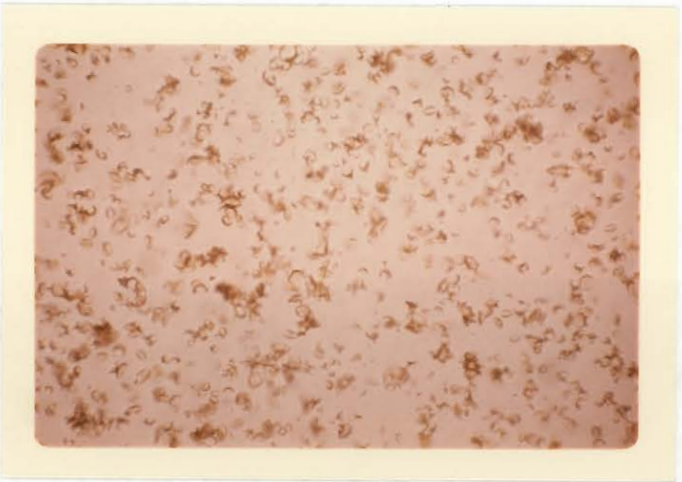

Fig. 17

Above Nylon microcapsules: mean diameter of microcapsules in batch about 90 μ, but the three shown here have diameters of about 250 μ. Left, in water; right, shortly after being placed in hypertonic saline. Magnification 60X.

Below Smaller Nylon microcapsules after crenation in hypertonic saline. Magnification 60X. (Compare with Fig. 3a, at the same magnification, which shows microcapsules of the same batch before crenation.

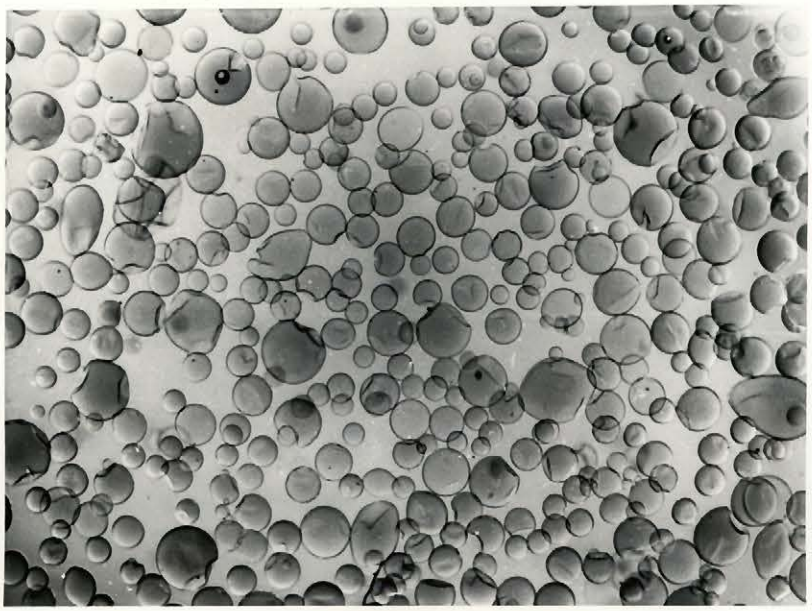

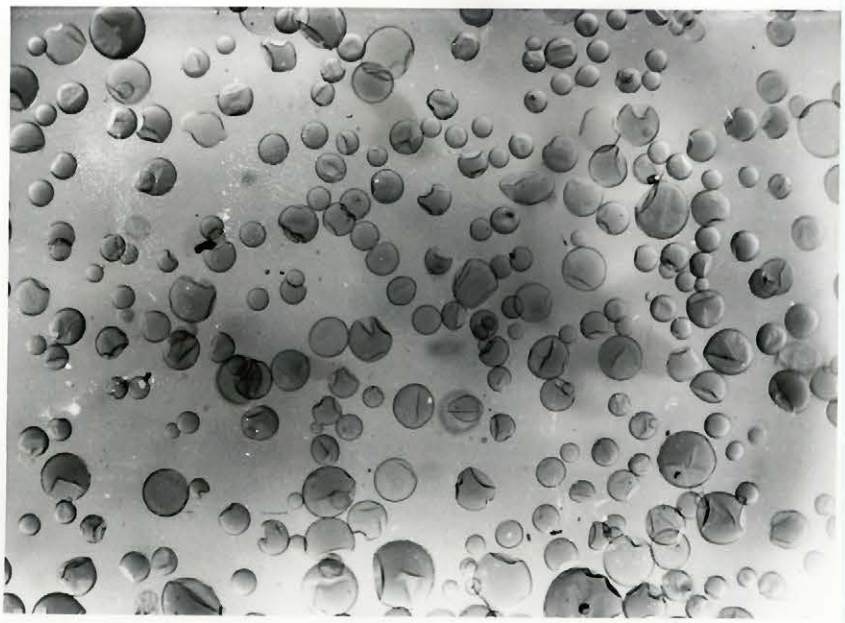

Fig. 19

Varying degrees of crenation of Nylon microcapsules (mean diameter 27 μ) 1 minute after exposure to hypertonic solutions of different concentrations.

(A) Proportion of crenated microcapsules was determined by counting to be 45 %.

(B) Proportion of crenated microcapsules was determined by counting to be 72 %.